

Supporting information for

Deconvoluting nitric oxide-protein interactions with spatial-resolved multiplex imaging

Yi Li, Kaijun Pan, Yanan Gao, Jia Li, Yi Zang, Xin Li

Table of contents

- Figure S1.** Protein-interaction-induced fluorogenic response of SiR-COOH derivatives.
- Figure S2.** Verification of the reaction between **NOP-1** and NO by LC-MS.
- Figure S3.** NO-dose-dependent labeling of FBS by **NOP-1**.
- Figure S4.** Time-dependent labeling of FBS by **NOP-1** in the presence of NO.
- Figure S5.** **NOP-1** labeled FBS only in the presence of NO.
- Figure S6.** NO-dose-dependent labeling of HepG2 cell lysates by **NOP-1**.
- Figure S7.** Time-dependent labeling of HepG2 cell lysates by **NOP-1** in the presence of NO.
- Figure S8.** Confocal fluorescence imaging of **NOP-1** in 293T cells stimulated by exogenous NO.
- Figure S9.** Confocal fluorescence imaging of **NOP-1** in HT22 cells stimulated by exogenous NO.
- Figure S10.** The comparison between DAF-FM DA and **NOP-1** in monochrome staining.
- Figure S11.** Further confirming the protein-labeling ability of **NOP-1**.
- Figure S12.** Enlarged version for Figure 5C.
- Figure S13.** Enlarged version for Figure 5D.
- Figure S14.** Comparison of the **NOP-1** and NO₂-Tyr antibody labeling results on whole-cell lysis.

Experimental Details

Synthesis and Characterization of the Compounds

Spectra traces

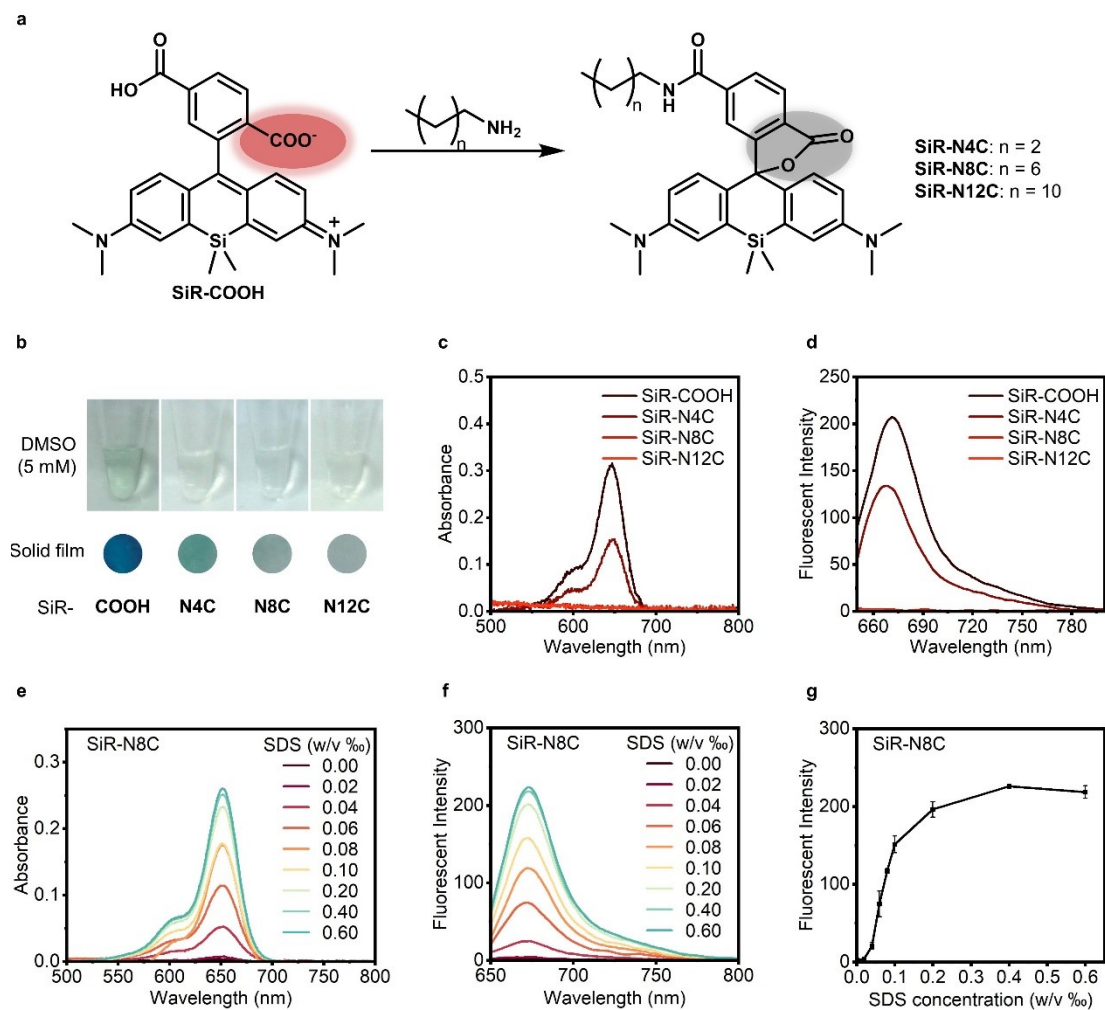


Figure S1. Protein-interaction-induced fluorogenic response of SiR-COOH derivatives. (a) Structures of SiR-COOH and its alkyl amide derivatives. (b) Images of SiR-COOH and its derivatives either dissolved in DMSO (5 mM) or as solids. (c, d) The absorption and fluorescence spectra of SiR-COOH and its derivatives (6 μ M) in PBS (10 mM, pH 7.4). (e, f) The absorption and fluorescence spectra of SiR-N8C (6 μ M) in PBS with various concentrations of SDS. (g) Plot of the fluorescent intensity of SiR-N8C at 672 nm versus the SDS concentrations. Error bars represent the standard deviation (SD) ($n = 3$).

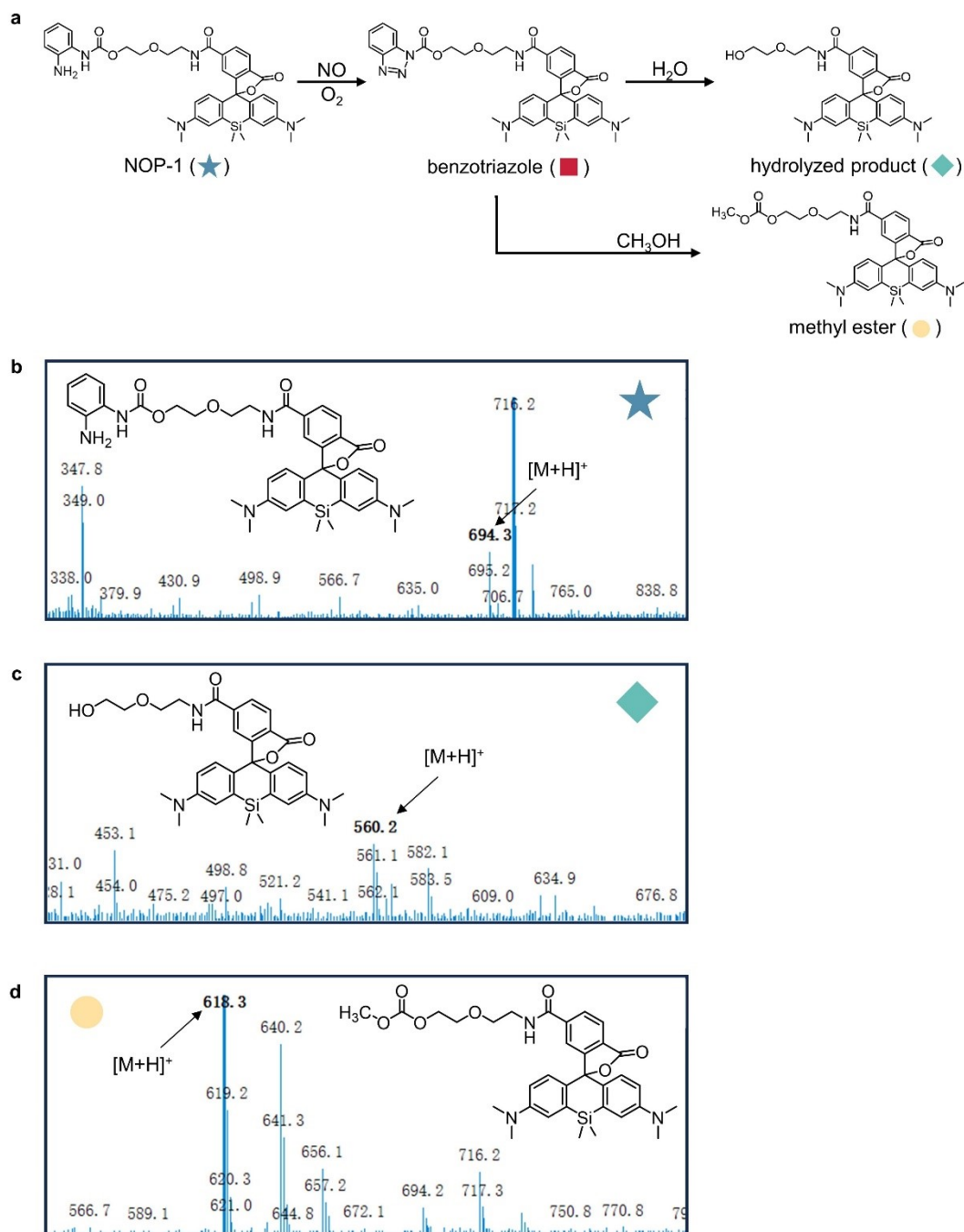


Figure S2. Verification of the reaction between **NOP-1** and NO by Liquid Chromatography-Mass Spectrometry (LC-MS). (a) Scheme of the NO-triggered reaction mechanism and subsequent hydrolysis and methyl esterization. (b) Mass spectrum of the peak at 8.990 min before reaction which was assigned to the molecular weight of **NOP-1**. (c) Mass spectrum of the peak at 8.482 min after 30-min reaction, which was attributed to the hydrolyzed product. (d) Mass spectrum of the peak at 8.922 min after 30 min's reaction, which was attributed to the methyl esterized product.

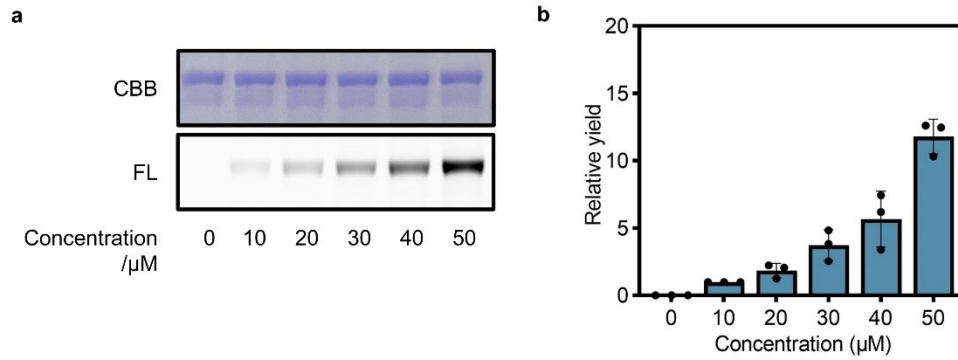


Figure S3. NO-dose-dependent labeling of FBS by **NOP-1**. (a) In-gel fluorescence analysis of FBS (0.4 mg/mL) incubated with **NOP-1** (1 μ M) and DEA-NONOate (0-50 μ M) at 37 $^{\circ}$ C for 60 min. The upper panel shows an image of the Coomassie Brilliant Blue (CBB)-stained gel while the lower panel shows an image of in-gel fluorescence scanning. (b) Quantification of labeling yield of bands in (a). Signal intensity was normalized to protein concentration as measured by CBB and to the data of the 10 μ M DEA-NONOate group. Error bars represent the SD (n = 3).

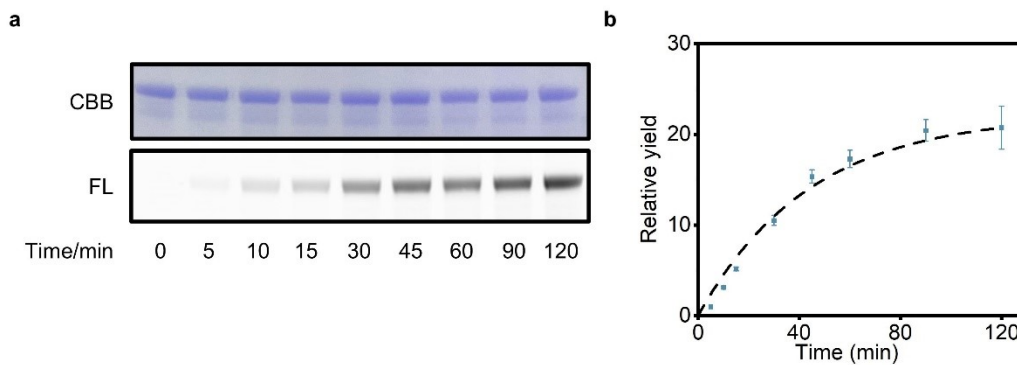


Figure S4. Time-dependent labeling of FBS by **NOP-1** in the presence of NO. (a) In-gel fluorescence analysis of FBS (0.4 mg/mL) incubated with **NOP-1** (1 μ M) and DEA-NONOate (50 μ M) at 37 $^{\circ}$ C for 0-120 min. The upper panel shows an image of the CBB-stained gel while the lower panel shows an image of in-gel fluorescence scanning. (b) Quantification of labeling yield of bands in (a). Signal intensity was normalized to protein concentration as measured by CBB and to the data of the 5 min group. The black dashed curve represents the fitted relationship between the relative labeling yield and the incubation time. Error bars represent the SD (n = 3).

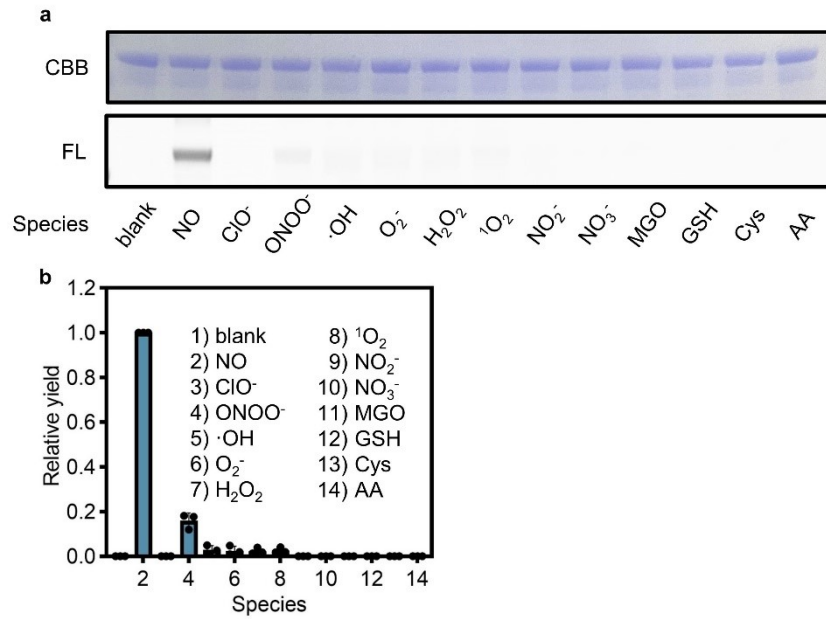


Figure S5. **NOP-1** labeled FBS only in the presence of NO. (a) In-gel fluorescence analysis of FBS (0.4 mg/mL) incubated with **NOP-1** (1 μ M) and various species at 37 °C for 60 min. The upper panel shows an image of the CBB-stained gel while the lower panel shows an image of in-gel fluorescence scanning. (b) Quantification of labeling yield of bands in (a). Signal intensity was normalized to protein concentration as measured by CBB and to the data of the NO group. Error bars represent the SD (n = 3).

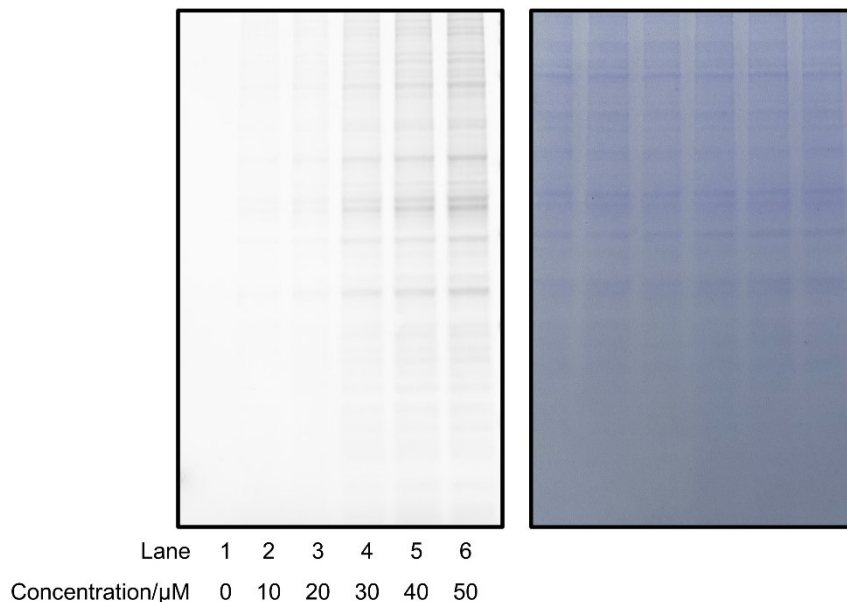


Figure S6. NO-dose-dependent labeling of HepG2 cell lysates by **NOP-1**. In-gel fluorescence analysis of HepG2 cell lysis (0.32 mg/mL) incubated with **NOP-1** (1 μ M) and DEA-NONOate (0-50 μ M) at 37 °C for 60 min. The left panel shows an image of in-gel fluorescence scanning while the right panel shows an image of the CBB-stained gel.

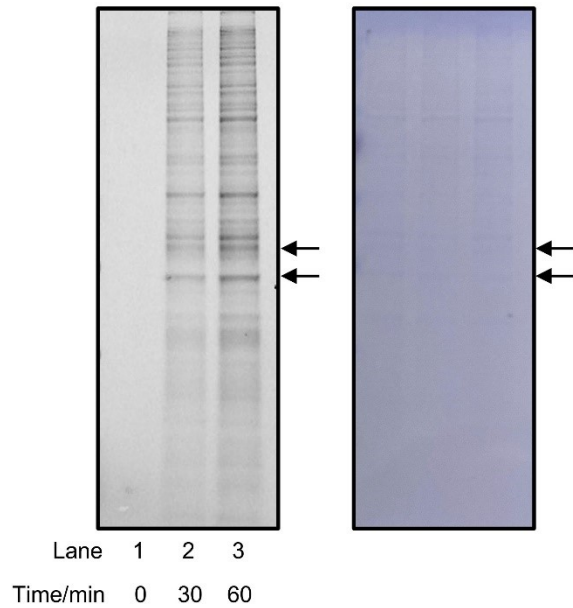


Figure S7. Time-dependent labeling of HepG2 cell lysates by **NOP-1** in the presence of NO. In-gel fluorescence analysis of HepG2 cell lysates (0.32 mg/mL) incubated with **NOP-1** (1 μ M) and DEA-NONOate (50 μ M) at 37 $^{\circ}$ C for 0-60 min. The left panel shows an image of in-gel fluorescence scanning while the right panel shows an image of the CBB-stained gel. The arrows highlight some bands that could be visible only by in-gel fluorescence scanning but almost invisible by CBB staining.

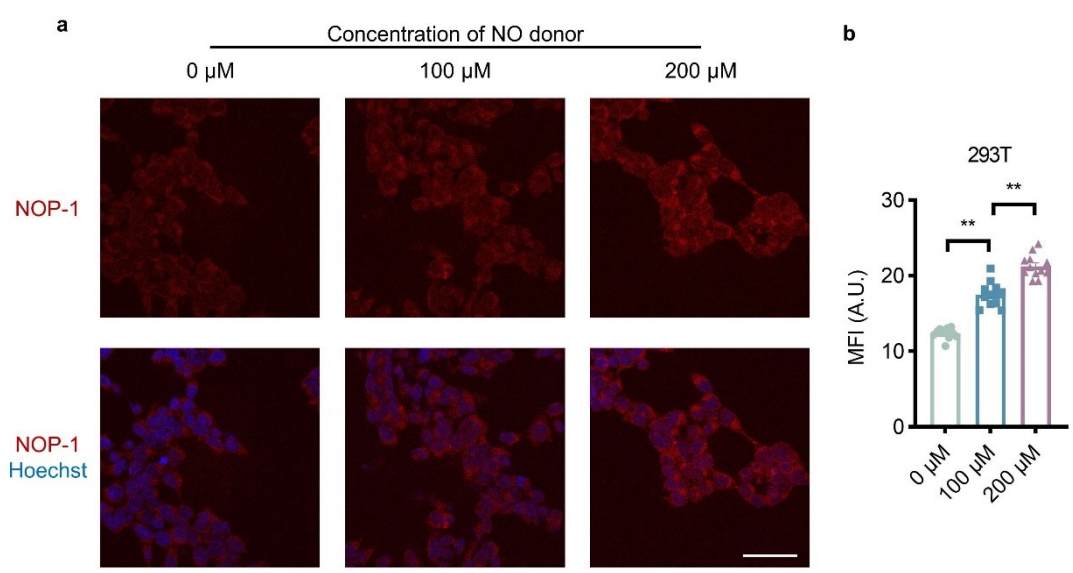


Figure S8. Confocal fluorescence imaging of 293T cells stimulated by different concentrations of DEA-NONOate and stained with **NOP-1**. (a) 293T cells were pretreated with DEA-NONOate (0, 100, 200 μ M) for 30 min, followed by incubation with **NOP-1** (1 μ M) for 20 min. IF signals of **NOP-1**: red;

Hoechst: blue. Scale bar = 50 μm . (b) Relative red fluorescence intensity output of (a). Error bars represent SD. The experiment was repeated three times. * $p < 0.05$; ** $p < 0.01$.

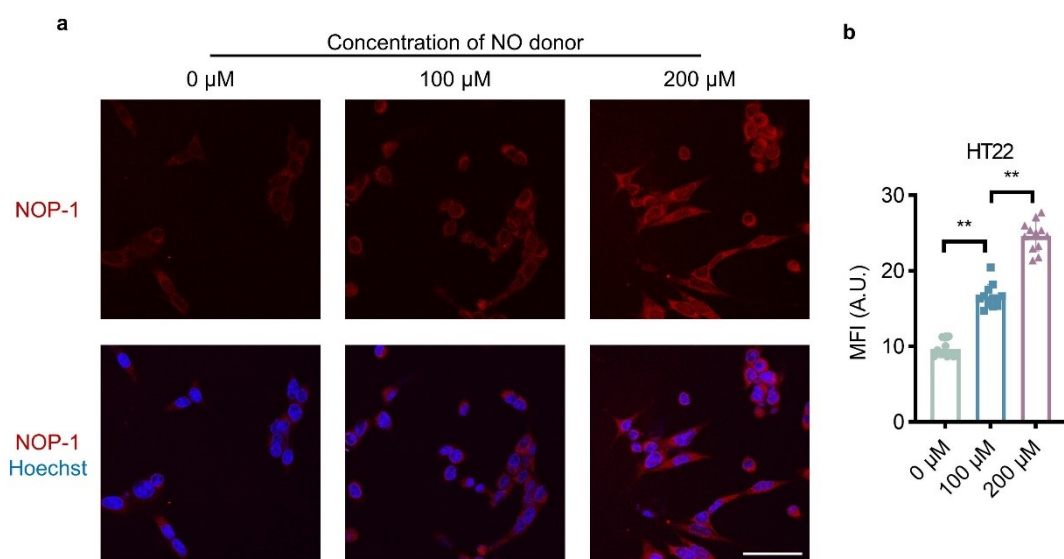


Figure S9. Confocal fluorescence imaging of HT22 cells stimulated by different concentrations of DEA-NONOate and stained with **NOP-1**. (a) HT22 cells were pretreated with DEA-NONOate (0, 100, 200 μM) for 30 min, followed by incubation with **NOP-1** (1 μM) for 20 min. IF signals of **NOP-1**: red; Hoechst: blue. Scale bar = 50 μm . (b) Relative red fluorescence intensity output of (a). Error bars represent SD. The experiment was repeated three times. * $p < 0.05$; ** $p < 0.01$.

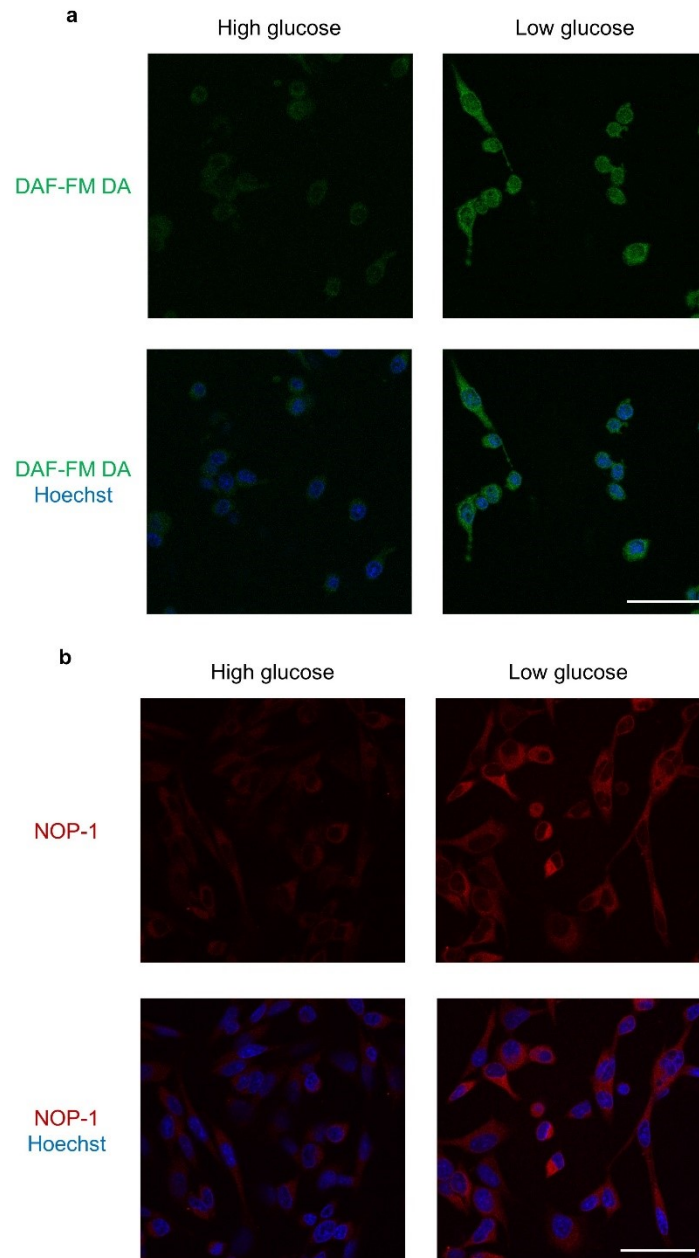


Figure S10. The comparison between a commercial probe DAF-FM DA (a) and **NOP-1** (b) in monochrome staining. HT22 cells were treated with high-glucose or low-glucose medium for 6 h, followed by incubation with DAF-FM DA or **NOP-1** (1 μ M) for 20 min. (a) IF signals of DAF-FM DA: green; Hoechst: blue. Scale bar = 50 μ m. (b) IF signals of **NOP-1**: red; Hoechst: blue. Scale bar = 50 μ m. The experiment was repeated three times for either group.

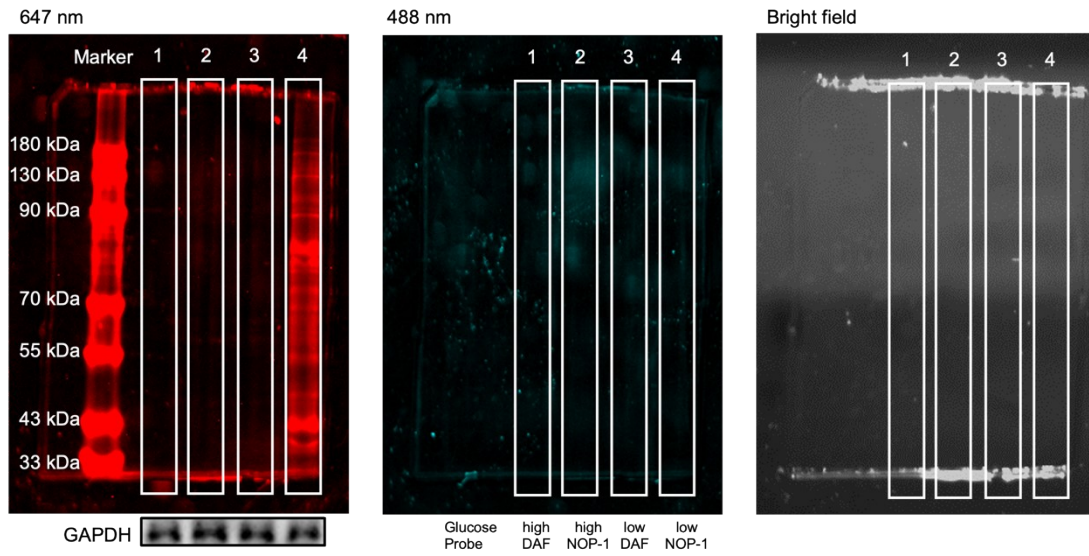


Figure S11. Further confirming the protein-labeling ability of NOP-1.

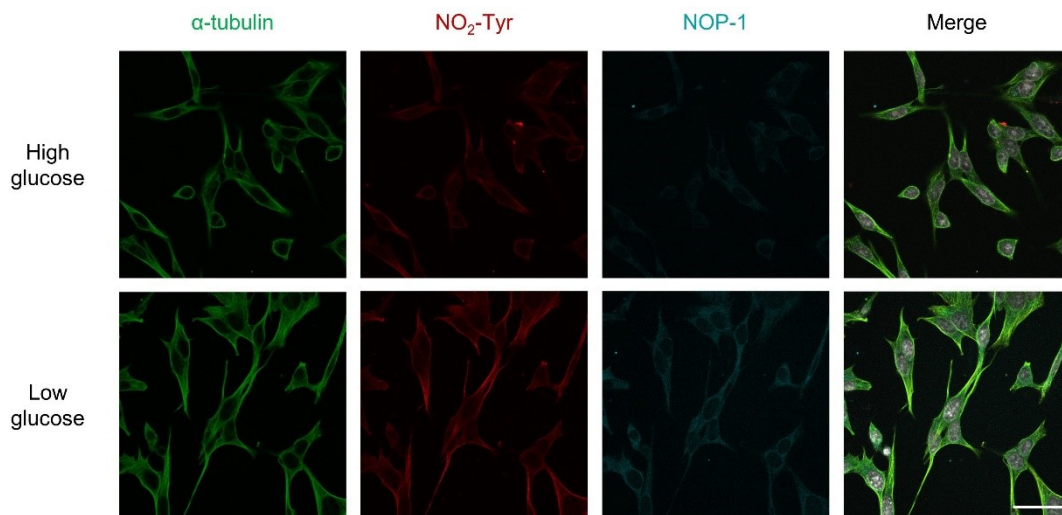


Figure S12. Enlarged version for Figure 5C. Scale bar = 50 μm .

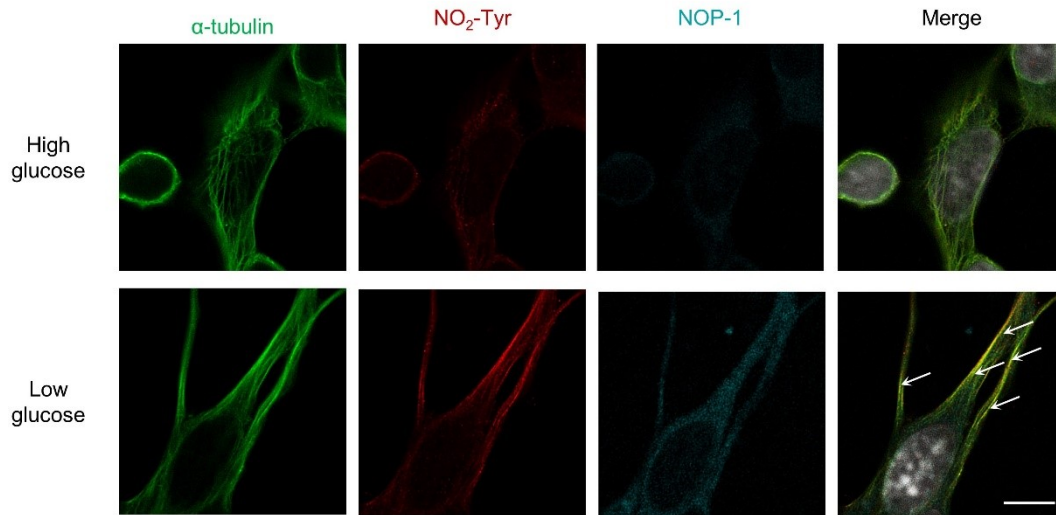


Figure S13. Enlarged version for Figure 5D. Scale bar = 50 μm .

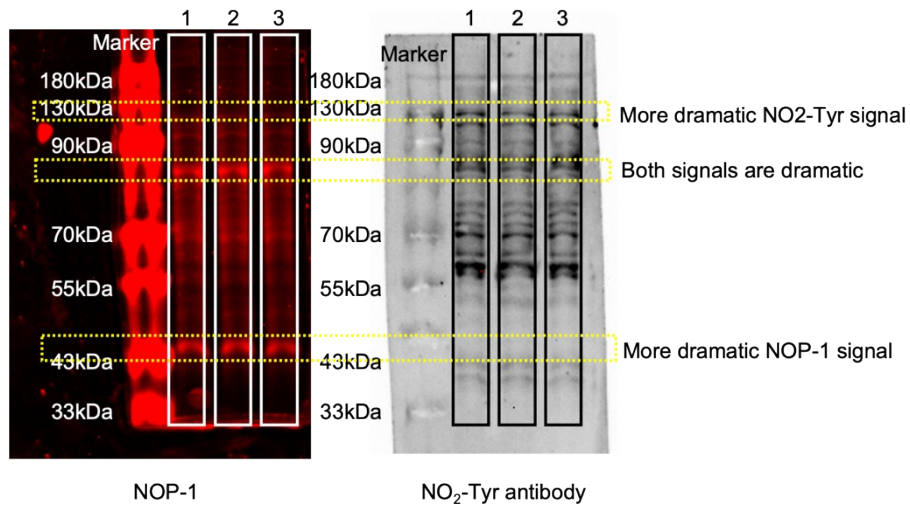


Figure S14. Comparison of the **NOP-1** and $\text{NO}_2\text{-Tyr}$ antibody labeling results on whole-cell lysis.

General materials and methods for the chemistry experiments

Reagents were purchased from commercial sources and used without further purification unless otherwise noted. Thin-layer chromatography (TLC) analysis of reactions was performed using Merck silica gel 60 F254 TLC plates and visualized using UV or Iodine staining.

^1H NMR spectra were recorded on a Bruker 500 Fourier transform spectrometer (500 MHz). ^{13}C NMR spectra were recorded on a Bruker 500 Fourier transform spectrometer (126 MHz). Sample concentrations for the NMR experiment were random. The residual solvent signals were used as references for ^1H and ^{13}C NMR spectra and the chemical shifts were converted to the TMS scale (CDCl_3 , 7.26 ppm for ^1H NMR and 77.16 ppm for ^{13}C NMR; CD_3OD , 3.31 ppm for ^1H NMR and 49.00 ppm for ^{13}C NMR). All chemical shifts were reported in parts per million (ppm) and coupling constants (J) in Hz. The following abbreviations were used to explain the multiplicities: d = doublet, t = triplet, m = multiplet, dd = doublet of doublets. High-resolution mass spectra (HRMS) for new compounds were measured on an Agilent 6224 TOF LC/MS spectrometer using ESI-TOF (electrospray ionization-time of flight). Protein mass spectral analyses were conducted using Bruker Ultraflex extreme MALDI-TOF/TOF.

Preparation of stock solutions

The alkyl amide derivatives of SiR-COOH and **NOPs** were dissolved in DMSO to make stock solutions of 5 mM. DEA-NONOate (Santa Cruz Biotechnology) was dissolved in 0.01 M NaOH aqueous solution to prepare a NO-donor stock solution of 10 mM.

Measurement of absorption and fluorescence spectra

The stock solutions of SiR-COOH and its derivatives were diluted to 6 μM with PBS (10 mM, pH 7.4). The UV-vis spectra were taken on a HITACHI U-3010 spectrophotometer. The fluorescence emission spectra were recorded using an Agilent Cary Eclipse fluorescence spectrophotometer, excited at 645 nm and scanned from 650 to 800 nm with slit widths of 2.5 nm for both excitation and emission.

For measurement of fluorogenic signals induced by NO-triggered protein labeling, the stock solutions of **NOPs** were diluted to 50 μM with PBS, or with Bovine serum albumin (BSA, 25 mg/mL) (Sigma-Aldrich, A1933) in PBS, or with a mixture of BSA (25 mg/mL) and DEA-NONOate (500 μM) in PBS. After incubation at 37 $^\circ\text{C}$ for 60 min, samples were diluted 10 \times with PBS, transferred to a 96-well plate, and scanned from 650 nm to 700 nm on a PECAN Spark Multifunctional Microplate Reader. $\lambda_{\text{ex}} = 600$ nm. Interrogation time was 40 μs . Gain = 75.

Protein labeling *in vitro*

To evaluate the NO-triggered protein labeling by the probes, BSA was first used as the model protein. **NOPs** (1 μM) were added to BSA (0.5 mg/mL) in PBS and incubated with indicated concentrations of DEA-NONOate at 37 $^\circ\text{C}$ for the indicated duration. For measurement of NO-selective labeling, **NOP-1** (1 μM) was added to BSA (0.5 mg/mL) in PBS and incubated with DEA-NONOate or other related species at 37 $^\circ\text{C}$ for 60 min. The final concentration was 50 μM for DEA-NONOate, 2 μM for ONOO $^-$, 100 μM for ClO^- , 500 μM for $\cdot\text{OH}$ and $^1\text{O}_2$, and 1 mM for the other species.

FBS was next used to assess the protein labeling ability of **NOP-1**. **NOP-1** (1 μM) was added to FBS (0.4 mg/mL) (Newzerum) in PBS and incubated with indicated concentrations of DEA-NONOate at 37 $^\circ\text{C}$ for the indicated duration. For measurement of NO-selective labeling, **NOP-1** (1 μM) was added to

FBS (0.4 mg/mL) in PBS and incubated with DEA·NONOate or other related species at 37 °C for 60 min. The final concentration was the same as in the case of BSA.

HepG2 cell lysates were then used as a more complicated system. To prepare cell lysates, HepG2 cells were rinsed with pre-cooled PBS, lysed with RIPA lysis buffer (Beyotime, P0013B) supplemented with PMSF (1 mM, Beyotime, ST506) on ice for 30 min, and centrifuged (12000 rpm at 4 °C for 5 min). The supernatant was collected, and the protein concentration was measured by BCA assay (Beyotime, P0012). **NOP-1** (1 μM) was added to lysates (0.32 mg/mL) dissolved in PBS and incubated with indicated concentrations of DEA·NONOate at 37 °C for the indicated duration.

After incubation, the resulting protein mixture was added with 5× loading buffer (Yeasten, 20315ES), boiled at 95 °C for 10 min and then centrifuged (15000 rpm at 4 °C for 45 s), followed by separation on 10% SDS-PAGE gels (Yeasten, 36252ES) using Bio-Rad PowerPac Basic 164505 and Bio-Rad Mini-PROTEAN® Tetra Cell, 4-Gell System 1658004, and scanning using GE Typhoon FLA 9500 multi-functional laser imager ($\lambda_{\text{ex}} = 635 \text{ nm}$, laser intensity = 1000 V). The total protein level on the gel was imaged by Coomassie Brilliant Blue staining. The integrated intensities of protein gels were analyzed by ImageJ.

Preparation of various species for the selectivity experiment

ClO⁻ was prepared by diluting commercial NaClO solution with PBS to make a stock solution of 10 mM.

H₂O₂ was prepared by diluting commercial H₂O₂ solution with PBS to make a stock solution of 100 mM.

ONOO⁻ was prepared using the following procedures. HCl (0.6 M, 10 mL) was added to a vigorously stirring mixture of H₂O₂ (0.7 M, 10 mL) and NaNO₂ (0.6 M, 10 mL) on ice followed by rapid addition of NaOH (1.5 M, 20 mL). Excessive H₂O₂ was removed by filtering the solution with MnO₂. The concentration of ONOO⁻ was determined by UV analysis with the extinction coefficient at 302 nm ($\epsilon = 1670 \text{ M}^{-1} \text{ cm}^{-1}$). Aliquots of the solution were stored at -20 °C for use.

·OH was generated by the Fenton reaction. A solution of H₂O₂ (100 mM, 1.0 mL) in PBS was added to a FeSO₄ solution (100 mM, 1.0 mL) at ambient temperature to make a stock solution of 50 mM.

¹O₂ was generated by adding a Na₂MoO₄ solution (100 mM, 1.0 mL) to a solution of H₂O₂ (100 mM, 1.0 mL) in PBS.

O₂⁻, NO₂⁻, NO₃⁻, MGO, GSH, Cys, AA were prepared by dissolving commercial KO₂, NaNO₂, NaNO₃, Methylglyoxal, Glutathione, L(+)-Cysteine, Ascorbic acid product in PBS to make stock solutions of 100 mM.

Cell culture

Human hepatocellular carcinoma cell line HepG2 cells, human embryonic kidney-derived cell line 293T cells, and mouse hippocampal cell line HT22 cells (ATTC, Rockville, MD, USA) were cultured in DMEM medium (Thermo Fisher Scientific) containing 10% FBS (Gibco) and 1% penicillin/streptomycin under a humidified atmosphere of 5% CO₂ in air at 37 °C. To evaluate the labeling performance of **NOP-1** under hypoglycemic conditions, 293T cells and HT22 cells were rinsed with fresh medium and then stimulated with a low-glucose (1 mM) medium for the indicated duration.

Protein labeling in response to exogenous NO in 293T and HT22 cells

293T cells and HT22 cells were incubated with DEA-NONOate (0, 100, 200 μM) for 30 min, followed by treatment with **NOP-1** (1 μM) for 20 min. The cells were washed with PBS for five times and then fixed with cold methanol. The cells were imaged by confocal microscopy (Leica SP8) and cellular fluorescence intensity was analyzed (**NOP-1** channel: $\lambda_{\text{ex}} = 635 \text{ nm}$, $\lambda_{\text{em}} = 670 \text{ nm}$; Hoechst channel: $\lambda_{\text{ex}} = 350 \text{ nm}$, $\lambda_{\text{em}} = 461 \text{ nm}$).

Fluctuation of NO levels in hypoglycemia

In the study of temporal variation of NO levels in hypoglycemia, HT22 cells were incubated in low-glucose (1 mM) medium for 0, 3, 6, 9, and 12 h, followed by treatment with **NOP-1** (1 μM) for 20 min. To confirm the fluctuation of NO levels, HT22 cells were incubated in low-glucose (1 mM) medium for 0, 3, 6, 9, and 12 h, followed by treatment with DAF-FM DA (1 μM) for 20 min. The cells were washed with PBS for five times and then fixed with cold methanol. The cells were imaged by confocal microscopy (Leica SP8) and cellular fluorescence intensity was analyzed. (**NOP-1** channel: $\lambda_{\text{ex}} = 635 \text{ nm}$, $\lambda_{\text{em}} = 670 \text{ nm}$; DAF-FM DA channel: $\lambda_{\text{ex}} = 495 \text{ nm}$, $\lambda_{\text{em}} = 515 \text{ nm}$; Hoechst channel: $\lambda_{\text{ex}} = 350 \text{ nm}$, $\lambda_{\text{em}} = 461 \text{ nm}$).

TUNEL assay

In the study of apoptosis, HT22 cells were pretreated with L-NMMA (100 μM) (MCE, HY-18732A), followed by incubation in a high-glucose medium or low-glucose (1 mM) medium for 6 h and fixation with cold methanol. The apoptotic cells were analyzed by TUNEL assay. Briefly, the TUNEL assay uses terminal deoxynucleotidyl transferase (TdT) to connect deoxynucleotides with fluorescent dyes, or other markers to the 3'-hydroxyl end of DNA double-strand breaks. The nucleotides are directly coupled with fluorescent dyes FITC, and then analyzed by optical microscopy (OLYMPUS, IX71) (FITC channel: $\lambda_{\text{ex}} = 490 \text{ nm}$, $\lambda_{\text{em}} = 525 \text{ nm}$; Hoechst channel: $\lambda_{\text{ex}} = 350 \text{ nm}$, $\lambda_{\text{em}} = 461 \text{ nm}$).¹

Immunohistochemistry

HT22 cells were incubated with primary antibodies respectively against α -tubulin (1:800, abcam), NO_2 -Tyr (1:200) (Sigma-Aldrich), NeuN (1:200) (Millipore) overnight at 4 $^\circ\text{C}$ in PBS containing BSA (5%) (Sigma-Aldrich) and Triton X-100 (0.2%). After washing with PBS to move away unbound antibodies, the corresponding secondary antibody was added to the cells and incubated at room temperature for 1 or 2 h. The cells were then washed again with PBS, and treated with Hoechst 33342 (Beyotime) dissolved in PBS (1:3000 dilution) to visualize the nuclei of the cells. The cells were mounted with coverslips and allowed to be imaged by confocal microscopy (Leica SP8) (**NOP-1** channel: $\lambda_{\text{ex}} = 635 \text{ nm}$, $\lambda_{\text{em}} = 670 \text{ nm}$; DAF-FM DA channel: $\lambda_{\text{ex}} = 495 \text{ nm}$, $\lambda_{\text{em}} = 515 \text{ nm}$; Hoechst channel: $\lambda_{\text{ex}} = 350 \text{ nm}$, $\lambda_{\text{em}} = 461 \text{ nm}$; NeuN channel: $\lambda_{\text{ex}} = 555 \text{ nm}$, $\lambda_{\text{em}} = 565 \text{ nm}$; α -tubulin channel: $\lambda_{\text{ex}} = 488 \text{ nm}$, $\lambda_{\text{em}} = 495 \text{ nm}$; NO_2 -Tyr channel: $\lambda_{\text{ex}} = 555 \text{ nm}$, $\lambda_{\text{em}} = 565 \text{ nm}$).

Immunoprecipitation (IP)

HT22 cells were incubated in a low-glucose (1 mM) medium for 6 h, followed by treatment with **NOP-1** (1 μM) for 20 min. The cells were then lysed with IP cell lysis buffer (Beyotime, P0013) supplemented with a protease inhibitor cocktail (MCE, HY-K0010) and centrifuged (10000 rpm at 4 $^\circ\text{C}$

for 10 min). The supernatant was collected and mixed with an IgG control (1:100) (CST, 3900) or a NO₂-Tyr antibody (1:100) (Sigma-Aldrich, 06-284), followed by rotation at 4 °C overnight. Protein A agarose (Sigma Aldrich, P3476) was then added to the mixture and incubated at 4 °C for 2 h. The mixture was washed with ice-cold PBS at 1200 rpm for 10 min, and the supernatant was discarded. The precipitates (bead-antibody-protein complex) were washed with ice-cold PBS at 1200 rpm at 4 °C for five times. Precipitation was harvested by SDS-loading and detected by Western blot.

Comparison of the NOP-1 and DAF-FM DA labeling on whole-cell lysis.

HT22 cells were cultured in low-glucose (1 mM) or high-glucose medium for 6 h, and subsequently stained with **NOP-1** (5 μM) or DAF-FM DA (5 μM). The cells were then lysed with RIPA cell lysis buffer (Beyotime, P0013B) supplemented with a protease inhibitor cocktail (MCE, HY-K0010). The total protein concentration was determined by BCA assay. The samples were added with SDS loading buffer and analyzed by Western blot.

Comparison of the NOP-1 and NO₂-Tyr antibody labeling on whole-cell lysis.

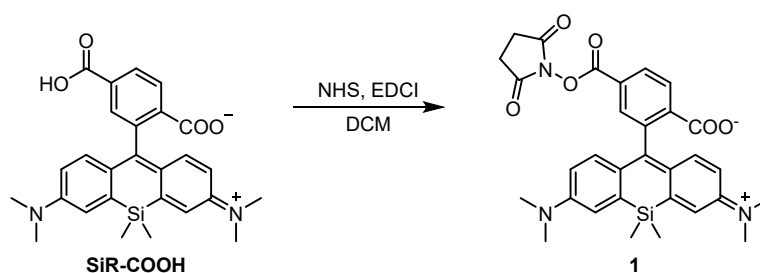
HT22 cells were cultured in low-glucose (1 mM) medium for 6 h, and subsequently stained with **NOP-1** (5 μM). The cells were then lysed with RIPA cell lysis buffer (Beyotime, P0013B) supplemented with a protease inhibitor cocktail (MCE, HY-K0010). The total protein concentration was determined by BCA assay. The samples were added with SDS loading buffer and detected by Western blot.

Western blot

The samples were denatured by boiling with SDS at 95 °C for 10 min and then separated by SDS-PAGE with a gradient of 8% to 15% acrylamide. The proteins were then transferred to a PVDF membrane according to their molecular weight and blocked with either 5% skim milk or BSA at room temperature for 1 h. Afterwards, the membrane was washed with TBST for three times, and incubated with the corresponding primary antibody at 4 °C overnight, followed by washing with TBST for three times and incubation with the secondary antibody for 1 h. The membrane was then exposed to ECL detection buffer (Bio-Rad, 1705061) and imaged by the ChemiDoc system.

To compare **NOP-1** and DAF-FM DA labeling, the protein gel was first analyzed by the 488 nm channel, 647 nm channel, and bright field. The same gel was then transferred to a PVDF membrane, incubated with internal control antibody GAPDH (1:5000) (CST, 2118L), and the secondary antibody. To compare **NOP-1** and NO₂-Tyr antibody labeling, a part of the samples was separated by SDS-PAGE and then analyzed by the 647 nm channel. Another part of the samples was separated by SDS-PAGE, transferred to a PVDF membrane, incubated NO₂-Tyr antibody (1:300), and the secondary antibody. The gel or membrane were then exposed to ECL detection buffer and imaged by the ChemiDoc system.

Chemical synthesis



SiR-COOH was synthesized according to the literature.²

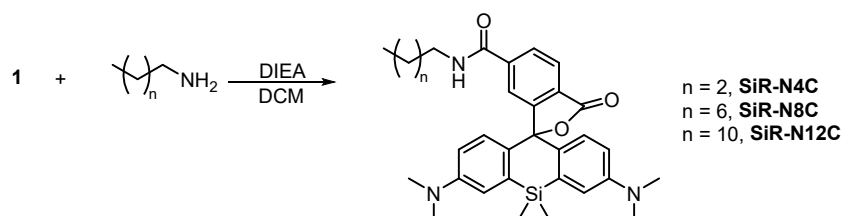
R_f = 0.30 (CH₂Cl₂/methanol = 15/1).

¹H NMR (500 MHz, Methanol-d₄) δ 8.21 (d, *J* = 8.0 Hz, 1H), 7.99 (d, *J* = 7.4 Hz, 1H), 7.85 (s, 1H), 7.04 (d, *J* = 2.8 Hz, 2H), 6.73 (d, *J* = 8.9 Hz, 2H), 6.63 (dd, *J* = 9.0, 2.9 Hz, 2H), 2.95 (s, 12H), 0.65 (s, 3H), 0.56 (s, 3H).

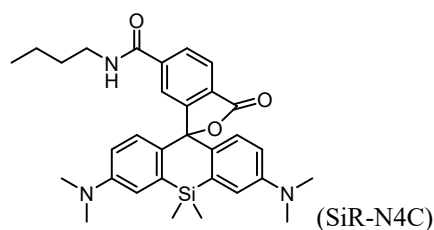
ESI-MS (*m/z*): [M+H]⁺ calc'd. for C₂₇H₂₉N₂O₄Si 473.1891, found 473.2.

1 was synthesized using the following procedures. SiR-COOH (75.0 mg, 0.159 mmol, 1.0 eq), N-Hydroxy succinimide (NHS) (27.0 mg, 0.238 mmol, 1.5 eq), 1-ethyl-3-(3-dimethylpropylamine)carbodiimide (EDCI) (46.0 mg, 0.238 mmol, 1.5 eq) was dissolved in dry dichloromethane (DCM) (800 μ L) and stirred at room temperature overnight. The reaction mixture was evaporated under reduced pressure and the residue was purified using silica gel column chromatography (PE/EA = 5/1 to 1/1) to obtain **1** as a chartreuse solid (51.0 mg, 56.3% yield). **1** was used for the next reaction immediately due to its instability.

Scheme S1. General procedures for synthesizing SiR-NCs



1 (0.0700 mmol, 1.0 eq) and the corresponding amine (0.0840 mmol, 1.2 eq) were dissolved in dry DCM (200 μ L) and stirred at room temperature for 10 min, followed by the addition of N, N-Diisopropylethylamine (DIEA) (0.140 mmol, 2.0 eq) and stirring at room temperature for 30 min. The resulting solution was evaporated under reduced pressure. The residue was purified using silica gel column chromatography to obtain **SiR-NCs** as a light-green solid.



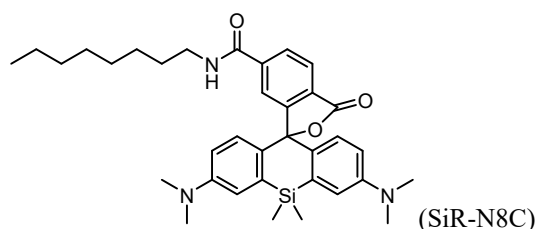
SiR-N4C was obtained as a brown oil after silica column chromatography (PE/EA = 2/1, 54.0% yield).

Rf = 0.50 (PE/EA = 1/1).

¹H NMR (500 MHz, Chloroform-d) δ 7.97 (dd, J = 7.9, 0.8 Hz, 1H), 7.91 (dd, J = 8.0, 1.4 Hz, 1H), 7.62 (s, 1H), 6.96 (d, J = 2.9 Hz, 2H), 6.77 (d, J = 8.9 Hz, 2H), 6.56 (dd, J = 9.0, 2.9 Hz, 2H), 6.20 (t, J = 5.8 Hz, 1H), 3.42 – 3.37 (m, 2H), 2.97 (s, 12H), 1.54 (t, J = 7.2 Hz, 2H), 1.39 – 1.34 (m, 2H), 1.26 (d, J = 2.1 Hz, 3H), 0.67 (s, 3H), 0.59 (s, 3H).

¹³C NMR (126 MHz, Chloroform-d) δ 170.13, 166.32, 155.48, 140.21, 136.80, 129.04, 125.98, 122.88, 92.13, 31.68.

ESI-HRMS (m/z): [M+H]⁺ calc'd. for C₃₁H₃₈N₃O₃Si 528.2677, found 528.2708.



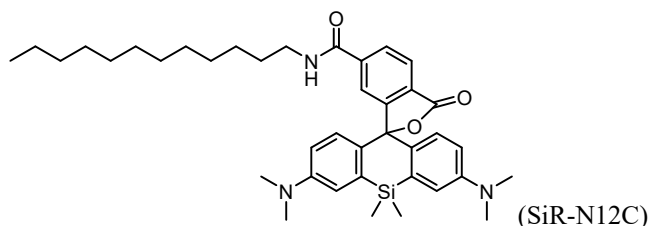
SiR-N8C was obtained as a brown oil after silica column chromatography (PE/EA = 5/1, 92.3% yield).

Rf = 0.35 (PE/EA = 2/1).

¹H NMR (500 MHz, Chloroform-d) δ 7.97 (dd, J = 8.0, 0.7 Hz, 1H), 7.92 – 7.90 (m, 1H), 7.61 (t, J = 1.0 Hz, 1H), 6.96 (d, J = 2.9 Hz, 2H), 6.77 (d, J = 8.9 Hz, 2H), 6.56 (dd, J = 9.0, 2.9 Hz, 2H), 6.17 (s, 1H), 3.38 (td, J = 7.3, 5.7 Hz, 2H), 2.97 (s, 12H), 1.55 (t, J = 7.1 Hz, 3H), 1.26 (s, 12H), 0.67 (s, 3H), 0.59 (s, 3H).

¹³C NMR (126 MHz, Chloroform-d) δ 170.12, 166.30, 155.51, 149.48, 140.22, 136.77, 131.26, 129.03, 125.98, 122.87, 92.08, 32.06, 31.90, 31.57, 30.33, 29.65, 27.11, 22.75, 14.21.

ESI-HRMS (m/z): [M+H]⁺ calc'd. for C₃₅H₄₆N₃O₃Si 584.3343, found 584.3303.



SiR-N12C was obtained as a brown oil after silica column chromatography (PE/EA = 2/1, 54.0% yield).

Rf = 0.25 (PE/EA = 2/1).

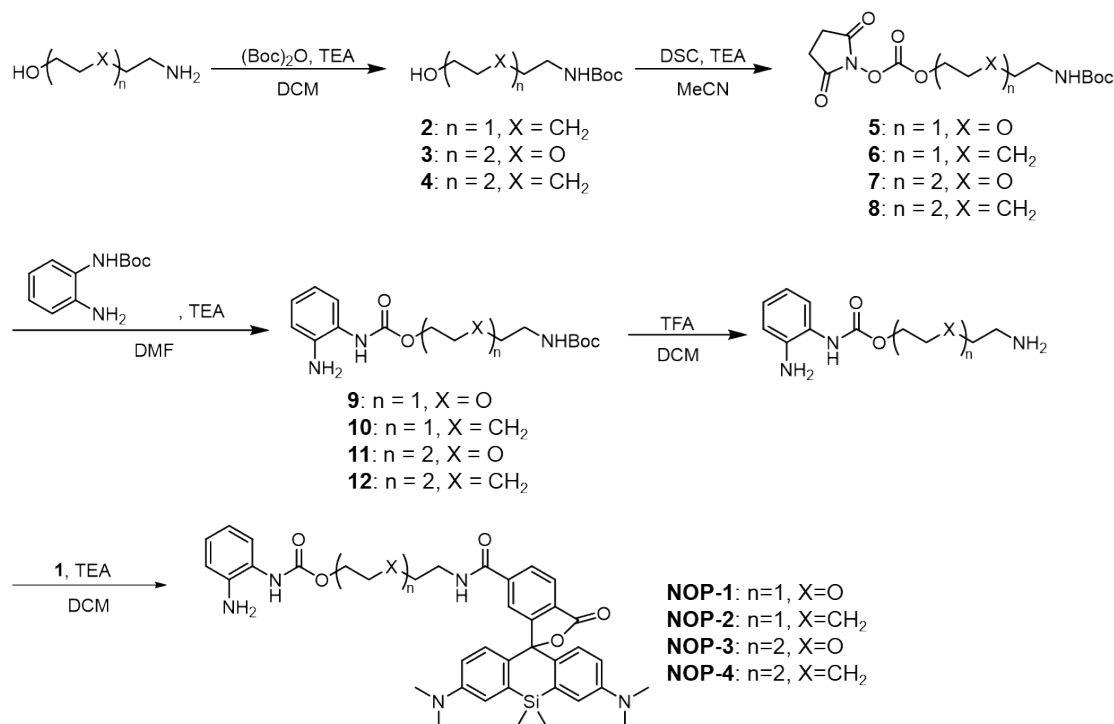
¹H NMR (500 MHz, Chloroform-d) δ 7.97 (d, J = 7.9 Hz, 1H), 7.90 (dd, J = 8.0, 1.4 Hz, 1H), 7.63 – 7.61 (m, 1H), 6.96 (d, J = 2.9 Hz, 2H), 6.77 (d, J = 8.9 Hz, 2H), 6.56 (dd, J = 9.0, 2.9 Hz, 2H), 6.20 (t, J = 5.7 Hz, 1H), 3.41 – 3.36 (m, 2H), 2.97 (s, 12H), 1.55 (t, J = 7.3 Hz, 3H), 1.25 (d, J = 7.4 Hz, 20H), 0.67 (s, 3H), 0.59 (s, 3H).

¹³C NMR (126 MHz, Chloroform-d) δ 170.13, 166.29, 155.49, 149.48, 140.22, 136.78, 131.24, 129.01,

125.97, 122.89, 92.11, 32.05, 32.03, 31.56, 29.83, 27.12, 22.81, 14.25.

ESI-HRMS (m/z): $[M+H]^+$ calc'd. for $C_{39}H_{54}N_3O_3Si$ 640.3929, found 640.3961.

Scheme S2. General procedures for synthesizing NOPs



The amino-alcohol (6.10 mmol, 1.0 eq) and $(Boc)_2O$ (6.10 mmol, 1.0 eq) were dissolved in dry DCM (15.0 mL) under nitrogen. The mixture was cooled to $0\text{ }^\circ\text{C}$ in an ice bath, followed by the addition of triethylamine (TEA) (7.32 mmol, 1.2 eq) and stirring at room temperature for 2 h. The reaction mixture was diluted with DCM and washed with saline, dried over Na_2SO_4 , then filtered and concentrated under reduced pressure. The residue was purified using a silica gel column chromatograph to obtain N-Boc-amino alcohol **2-4** as a pale-yellow oil.

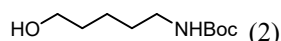
N-Boc-amino alcohol (4.01 mmol, 1 eq) was dissolved in dry MeCN (10 mL), cooled to $0\text{ }^\circ\text{C}$ in an ice bath, followed by the addition of TEA (8.02 mmol, 2.0 eq), and stirring at room temperature for 10 min. After adding N, N'-Disuccinimidyl carbonate (DSC) (8.02 mmol, 2.0 eq), the mixture was stirred at $40\text{ }^\circ\text{C}$ for 1 h. The reaction mixture was evaporated under reduced pressure. The residue was dissolved in EA and washed with saturated $NaHCO_3$ aqueous solution, water, and saline, dried over Na_2SO_4 , then filtered and concentrated under reduced pressure. The residue was purified using silica gel column chromatography to obtain active ester **5-8** as a colorless oil.

Active ester (2.38 mmol, 1.0 eq) and tert-butyl (2-aminophenyl)carbamate (3.57 mmol, 1.5 eq) were dissolved in dry DMF (5.00 mL), followed by the addition of TEA (7.15 mmol, 3.0 eq) and stirring at room temperature for 3 h. The reaction mixture was evaporated under reduced pressure. The residue was resolved in EA and washed with saline, dried over Na_2SO_4 , then filtered and concentrated under reduced pressure. The residue was purified using silica gel column chromatography to obtain OPD-attached linker **9-12** as a brown oil.

OPD-attached linker (0.18 mmol, 2.0 eq) was dissolved in DCM (2.00 mL), cooled to $0\text{ }^\circ\text{C}$ in ice bath, followed by the addition of trifluoroacetic acid (TFA) (1.00 mL) and stirring at room temperature for 1

h. The reaction mixture was evaporated under reduced pressure to obtain the intermediate as a brown oil which was used directly for the next reaction without further purification.

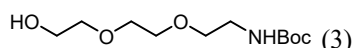
The residue and **1** (0.0900 mmol, 1.0 eq) were dissolved in dry DCM (700 μ L) and stirred at room temperature for 10 min, followed by the addition of DIEA (0.540 mmol, 6.0 eq) and stirring at room temperature for 30 min. The reaction mixture was evaporated under reduced pressure. The residue was purified using silica gel column chromatography **NOPs** as a light-green solid.



2 was obtained as a pale-yellow oil after silica column chromatography (PE/EA = 2/1, 92.4% yield). **Rf** = 0.35 (PE/EA = 1/1).

¹H NMR (500 MHz, Chloroform-*d*) δ 4.54 (s, 1H), 3.65 (t, *J* = 6.5 Hz, 2H), 3.13 (q, *J* = 6.7 Hz, 2H), 1.61 – 1.57 (m, 2H), 1.50 (q, *J* = 7.3 Hz, 2H), 1.44 (s, 9H), 1.42 – 1.39 (m, 2H).

ESI-MS (*m/z*): [M+Na]⁺ calc'd. for C₁₀H₂₁NNaO₃ 226.1414, found 226.1.

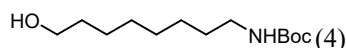


3 was obtained as a pale-yellow oil after silica column chromatography (DCM/methanol = 30/1, 87.5% yield).

Rf = 0.70 (DCM/methanol = 10/1).

¹H NMR (500 MHz, Chloroform-*d*) δ 5.13 (s, 1H), 3.74 (q, *J* = 5.1 Hz, 2H), 3.64 (t, *J* = 5.4 Hz, 4H), 3.60 (dd, *J* = 5.2, 3.8 Hz, 2H), 3.54 (t, *J* = 5.2 Hz, 2H), 3.31 (q, *J* = 5.5 Hz, 2H), 2.59 (s, 1H), 1.43 (s, 9H).

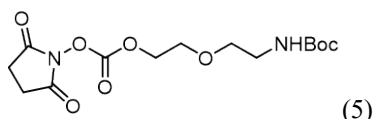
ESI-MS (*m/z*): [M+Na]⁺ calc'd. for C₁₁H₂₃NNaO₅ 272.1468, found 272.1.



4 was obtained as a pale-yellow oil after silica column chromatography (PE/EA = 1/1, 77.2% yield). **Rf** = 0.35 (PE/EA = 2/1).

¹H NMR (500 MHz, Chloroform-*d*) δ 4.53 (s, 1H), 3.62 (td, *J* = 6.7, 2.1 Hz, 2H), 3.08 (q, *J* = 7.0 Hz, 2H), 1.56 – 1.51 (m, 2H), 1.42 (s, 9H), 1.36 – 1.26 (m, 8H).

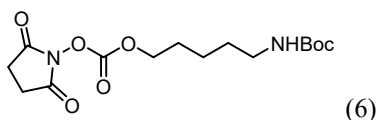
ESI-MS (*m/z*): [M+Na]⁺ calc'd. for C₁₃H₂₇NNaO₃ 268.1883, found 268.1.



5 was obtained as a white solid after silica column chromatography (PE/EA = 1/1, 66.4% yield). **Rf** = 0.50 (DCM/methanol = 30/1).

¹H NMR (500 MHz, Chloroform-*d*) δ 4.47 – 4.43 (m, 2H), 3.74 – 3.70 (m, 2H), 3.53 (d, *J* = 5.2 Hz, 2H), 3.31 (d, *J* = 5.7 Hz, 2H), 2.83 (s, 4H), 1.43 (s, 9H).

ESI-MS (*m/z*): [M+Na]⁺ calc'd. for C₁₄H₂₂N₂NaO₈ 369.1268, found 369.2.



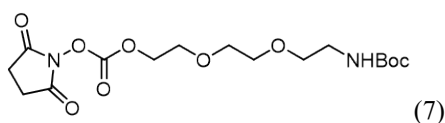
6 was obtained as a colorless oil after silica column chromatography (DCM/methanol = 100/1, 84.6% yield).

Rf = 0.55 (DCM/methanol = 30/1).

¹H NMR (500 MHz, Chloroform-*d*) δ 4.57 (s, 1H), 4.32 (t, *J* = 6.5 Hz, 2H), 3.12 (q, *J* = 6.7 Hz, 2H), 2.83 (s, 4H), 1.77 (dq, *J* = 8.0, 6.6 Hz, 2H), 1.65 (s, 2H), 1.55 – 1.49 (m, 2H), 1.43 (s, 9H).

¹³C NMR (126 MHz, Chloroform-*d*) δ 168.82, 156.13, 151.72, 71.48, 40.39, 29.72, 28.19, 25.60, 22.89.

ESI-HRMS (*m/z*): [2M+Na]⁺ calc'd. for C₃₀H₄₈N₄NaO₁₄ 711.3059, found 711.2922.



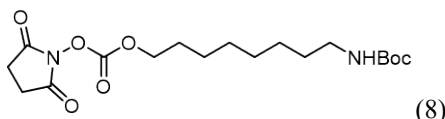
7 was obtained as a pale-yellow oil after silica column chromatography (DCM/methanol = 50/1, 76.7% yield).

Rf = 0.35 (DCM/methanol = 30/1).

¹H NMR (500 MHz, Chloroform-*d*) δ 5.02 (d, *J* = 6.0 Hz, 1H), 4.49 – 4.44 (m, 2H), 3.78 (dd, *J* = 4.0, 2.3 Hz, 2H), 3.67 – 3.59 (m, 4H), 3.53 (d, *J* = 5.3 Hz, 2H), 3.31 (q, *J* = 5.4 Hz, 2H), 2.83 (s, 4H), 1.42 (s, 9H).

¹³C NMR (126 MHz, Chloroform-*d*) δ 168.72, 156.20, 151.76, 79.34, 70.90, 68.47, 40.46.

ESI-HRMS (*m/z*): [M+Na]⁺ calc'd. for C₁₆H₂₆N₂NaO₉ 413.1531, found 413.1559.



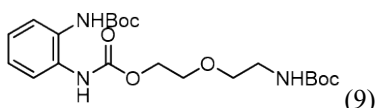
8 was obtained as a white solid after silica column chromatography (PE/EA = 5/1, 86.3% yield).

Rf = 0.70 (PE/EA = 1/1).

¹H NMR (500 MHz, Chloroform-*d*) δ 4.57 (s, 1H), 4.28 (t, *J* = 6.6 Hz, 2H), 3.06 (q, *J* = 6.7 Hz, 2H), 2.80 (s, 4H), 1.70 (p, *J* = 6.8 Hz, 2H), 1.44 (d, *J* = 7.7 Hz, 2H), 1.40 (s, 9H), 1.36 (t, *J* = 7.5 Hz, 2H), 1.28 (d, *J* = 4.2 Hz, 6H).

¹³C NMR (126 MHz, Chloroform-*d*) δ 168.84, 156.05, 151.66, 79.00, 71.63, 40.61, 30.05, 29.08, 28.99, 26.67.

ESI-HRMS (*m/z*): [M+Na]⁺ calc'd. for C₁₈H₃₀N₂NaO₇ 409.1945, found 409.1953.



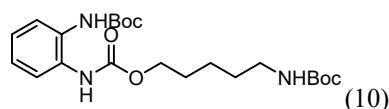
9 was obtained as a brown oil after silica column chromatography (DCM/methanol = 100/1, 72.3% yield).

Rf = 0.50 (DCM/methanol = 100/1).

¹H NMR (500 MHz, Chloroform-d) δ 7.51 (d, J = 20.7 Hz, 2H), 7.15 – 7.12 (m, 2H), 6.74 (s, 1H), 4.97 (s, 1H), 4.32 (dd, J = 4.1, 2.4 Hz, 2H), 3.71 (dd, J = 5.9, 3.3 Hz, 2H), 3.56 (t, J = 5.3 Hz, 2H), 3.33 (d, J = 6.4 Hz, 2H), 1.69 (s, 1H), 1.51 (s, 9H), 1.43 (s, 9H).

¹³C NMR (126 MHz, Chloroform-d) δ 156.16, 154.56, 153.98, 81.18, 79.55, 70.47, 69.34, 64.69, 40.49.

ESI-MS (m/z): $[M+Na]^+$ calc'd. for C₂₁H₃₃N₃NaO₇ 462.2211, found 462.2.



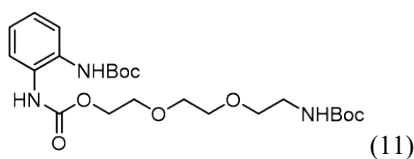
10 was obtained as a brown oil after silica column chromatography (PE/EA = 8/1, 89.8% yield).

R_f = 0.40 (PE/EA = 2/1).

¹H NMR (500 MHz, Chloroform-d) δ 7.55 – 7.41 (m, 2H), 7.13 (dd, J = 6.1, 3.5 Hz, 2H), 6.80 (s, 1H), 4.58 (s, 1H), 4.15 (t, J = 6.5 Hz, 2H), 3.12 (q, J = 6.9 Hz, 2H), 2.91 (d, J = 36.4 Hz, 1H), 1.75 – 1.63 (m, 4H), 1.51 (s, 9H), 1.43 (s, 9H), 1.40 (t, 2H).

¹³C NMR (126 MHz, Chloroform-d) δ 156.16, 154.92, 154.02, 125.61, 81.11, 79.31, 65.57, 40.52, 29.83, 23.39.

ESI-HRMS (m/z): $[M+Na]^+$ calc'd. for C₂₂H₃₅N₃NaO₆ 460.2418, found 460.2451.



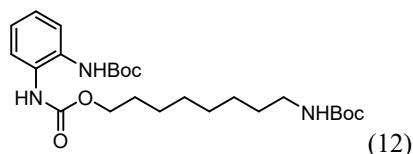
11 was obtained as a brown oil after silica column chromatography (DCM/methanol = 30/1, 83.4% yield).

R_f = 0.50 (DCM/methanol = 30/1).

¹H NMR (500 MHz, Chloroform-d) δ 7.45 (d, J = 24.7 Hz, 2H), 7.09 – 7.00 (m, 2H), 5.09 (s, 1H), 4.35 – 4.23 (m, 2H), 3.72 – 3.46 (m, 8H), 3.25 (q, J = 5.6 Hz, 2H), 1.47 (s, 9H), 1.39 (s, 9H).

¹³C NMR (126 MHz, Chloroform-d) δ 156.12, 154.56, 153.88, 125.31, 125.05, 80.69, 80.24, 79.30, 70.58, 70.24, 69.37, 64.44, 41.25, 40.38.

ESI-HRMS (m/z): $[M+Na]^+$ calc'd. for C₂₃H₃₇N₃NaO₈ 506.2473, found 506.2523.



12 was obtained as a brown oil after silica column chromatography (PE/EA = 8/1, 33.5% yield).

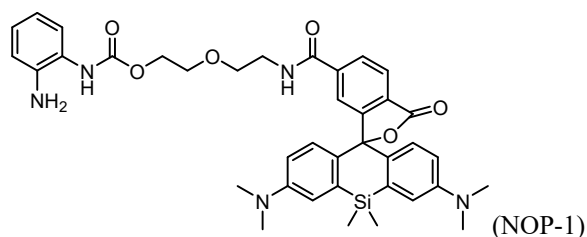
R_f = 0.50 (PE/EA = 2/1).

¹H NMR (500 MHz, Chloroform-d) δ 7.59 – 7.38 (m, 2H), 7.14 – 7.10 (m, 2H), 6.89 – 6.71 (m, 1H), 4.54 (s, 1H), 4.14 (t, J = 6.6 Hz, 2H), 3.09 (q, J = 6.8 Hz, 2H), 1.64 (q, J = 6.9 Hz, 2H), 1.51 (s, 9H), 1.47 (s, 2H), 1.44 (s, 9H), 1.36 – 1.26 (m, 8H).

¹³C NMR (126 MHz, Chloroform-d) δ 156.13, 154.93, 154.05, 125.59, 81.09, 79.17, 65.74, 40.72, 30.13,

29.19, 28.94, 26.77, 25.81.

ESI-HRMS (m/z): $[M+Na]^+$ calc'd. for $C_{25}H_{41}N_3NaO_6$ 502.2888, found 502.2935.



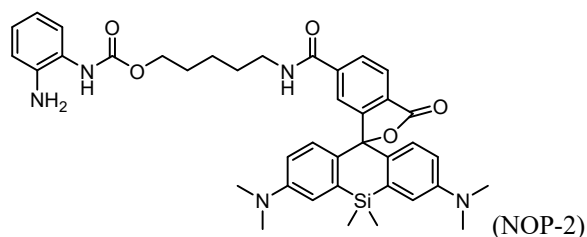
NOP-1 was obtained as a light-green solid after silica column chromatography (DCM/methanol = 20/1, 48.3% yield).

R_f = 0.35 (PE/EA = 1/1).

¹H NMR (500 MHz, Chloroform-*d*) δ 7.94 – 7.79 (m, 2H), 7.74 (s, 1H), 6.98 (t, J = 7.7 Hz, 1H), 6.94 (d, J = 2.9 Hz, 2H), 6.77 (s, 1H), 6.75 (s, 2H), 6.53 (dd, J = 9.0, 2.9 Hz, 2H), 4.29 (s, 1H), 3.73 – 3.55 (m, 8H), 2.94 (s, 12H), 1.85 (s, 4H), 0.65 (s, 3H), 0.59 (s, 3H).

¹³C NMR (126 MHz, Chloroform-*d*) δ 170.11, 166.50, 155.01, 149.47, 139.55, 136.93, 131.30, 128.19, 125.92, 123.52, 116.72, 113.49, 92.21, 69.68, 64.10, 29.82.

ESI-HRMS (m/z): $[M+H]^+$ calc'd. for $C_{38}H_{44}N_5O_6Si$ 694.3055, found 694.3079.



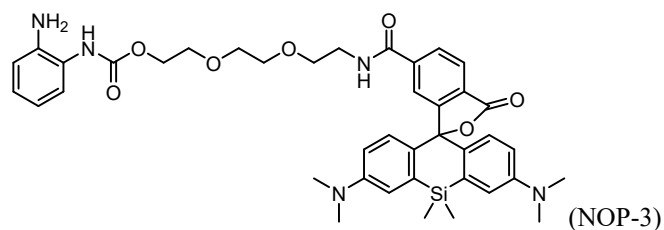
NOP-2 was obtained as a light-green solid after silica column chromatography (PE/EA = 1/2, 48.5% yield).

R_f = 0.40 (PE/EA = 1/2).

¹H NMR (500 MHz, Methanol-*d*₄) δ 8.02 – 7.97 (m, 2H), 7.66 (s, 1H), 7.11 (s, 1H), 7.03 (d, J = 3.0 Hz, 2H), 7.00 – 6.90 (m, 2H), 6.78 (d, J = 8.6 Hz, 1H), 6.71 (d, J = 8.9 Hz, 2H), 6.63 (dd, J = 9.0, 2.9 Hz, 2H), 4.11 (s, 1H), 2.95 (s, 12H), 1.66 (d, J = 36.7 Hz, 6H), 1.45 (s, 2H), 1.29 (s, 2H), 0.65 (s, 3H), 0.55 (s, 3H).

¹³C NMR (126 MHz, Methanol-*d*₄) δ 172.09, 151.16, 141.70, 137.82, 132.20, 129.16, 126.62, 124.48, 117.83, 114.93, 66.16, 54.81, 41.05, 40.48, 29.96, 29.77, 24.49.

ESI-HRMS (m/z): $[M+H]^+$ calc'd. for $C_{39}H_{46}N_5O_5Si$ 692.3263, found 692.3283.



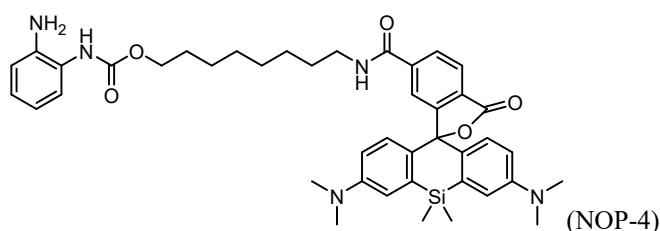
NOP-3 was obtained as a light-green solid after silica column chromatography (PE/EA = 1/3, 26.6% yield).

R_f = 0.40 (EA).

¹H NMR (500 MHz, Chloroform-*d*) δ 7.95 (d, *J* = 7.8, 1H), 7.92 (dd, *J* = 7.9, 1.4 Hz, 2H), 7.68 (s, 2H), 6.97 (dd, *J* = 7.8, 1.5 Hz, 1H), 6.95 (d, *J* = 3.0 Hz, 2H), 6.76 (d, *J* = 9.0 Hz, 2H), 6.67 (dd, *J* = 7.9, 1.4 Hz, 2H), 6.54 (dd, *J* = 8.9, 2.9 Hz, 2H), 4.20 – 4.18 (m, 2H), 3.66 – 3.57 (m, 12H), 2.96 (s, 12H), 1.69 (s, 4H), 0.66 (s, 3H), 0.59 (s, 3H).

¹³C NMR (126 MHz, Chloroform-*d*) δ 170.11, 166.60, 149.54, 139.89, 136.87, 131.39, 129.17, 128.32, 127.78, 125.92, 123.40, 116.72, 113.66, 92.15, 70.62, 70.29, 69.85, 69.47, 64.17.

ESI-HRMS (*m/z*): [M+H]⁺ calc'd. for C₄₀H₄₈N₅O₇Si 738.3330, found 738.3318.



NOP-4 was obtained as a light-green solid after silica column chromatography (PE/EA = 1/2, 35.0% yield).

R_f = 0.25 (PE/EA = 1/1).

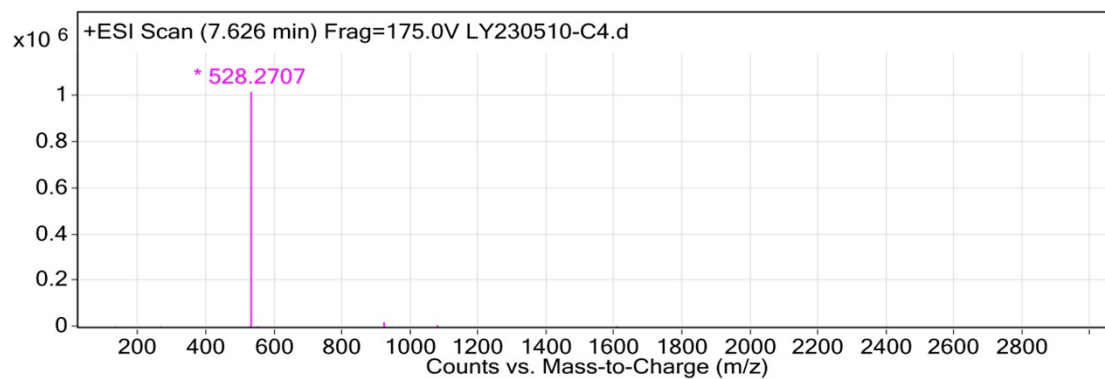
¹H NMR (500 MHz, Chloroform-*d*) δ 7.97 (d, *J* = 8.0 Hz, 1H), 7.89 (dd, *J* = 7.9, 1.5 Hz, 1H), 7.61 (s, 1H), 7.00 (td, *J* = 7.7, 1.5 Hz, 1H), 6.96 (d, *J* = 2.9 Hz, 2H), 6.77 (d, *J* = 9.0 Hz, 3H), 6.56 (dd, *J* = 9.0, 2.9 Hz, 2H), 6.22 (d, *J* = 5.5 Hz, 1H), 4.13 (t, *J* = 6.7 Hz, 2H), 3.73 (s, 2H), 3.38 (d, *J* = 13.6, 6.7 Hz, 2H), 2.96 (s, 12H), 1.64 (s, 4H), 1.56 (d, *J* = 8.5 Hz, 2H), 1.32 (s, 8H), 1.28 – 1.24 (m, 1H), 0.66 (s, 3H), 0.59 (s, 3H).

¹³C NMR (126 MHz, Chloroform-*d*) δ 170.13, 166.37, 155.50, 149.49, 140.17, 136.79, 131.25, 129.05, 128.32, 127.69, 126.00, 122.89, 116.63, 113.64, 92.09, 65.66, 53.57, 29.55, 28.96, 26.88, 25.81.

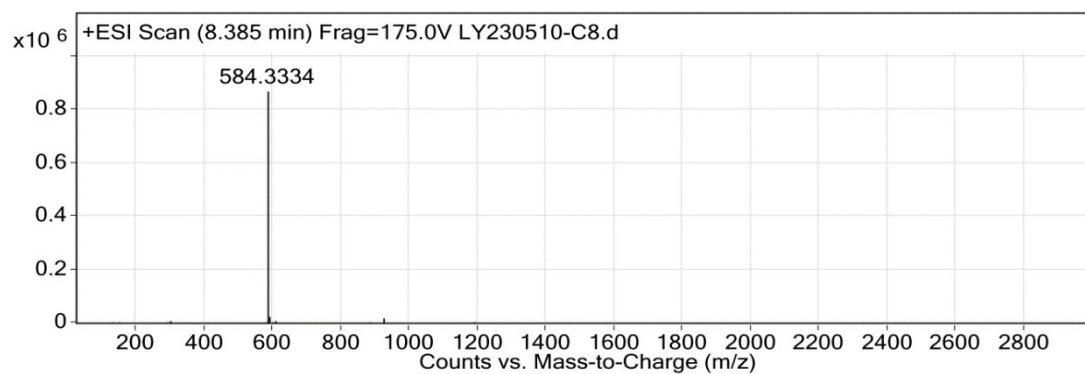
ESI-HRMS (*m/z*): [M+H]⁺ calc'd. for C₄₂H₅₂N₅O₅Si 734.3747, found 734.3732.

Spectra traces

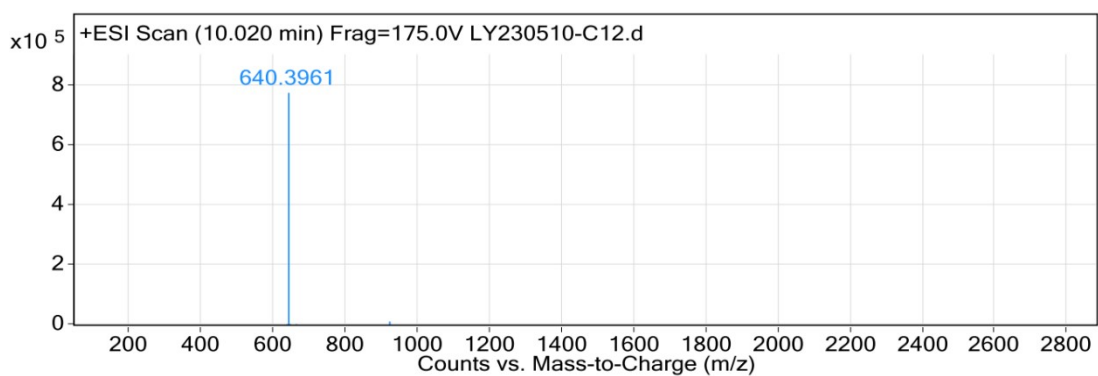
HRMS spectra of **SiR-N4C**



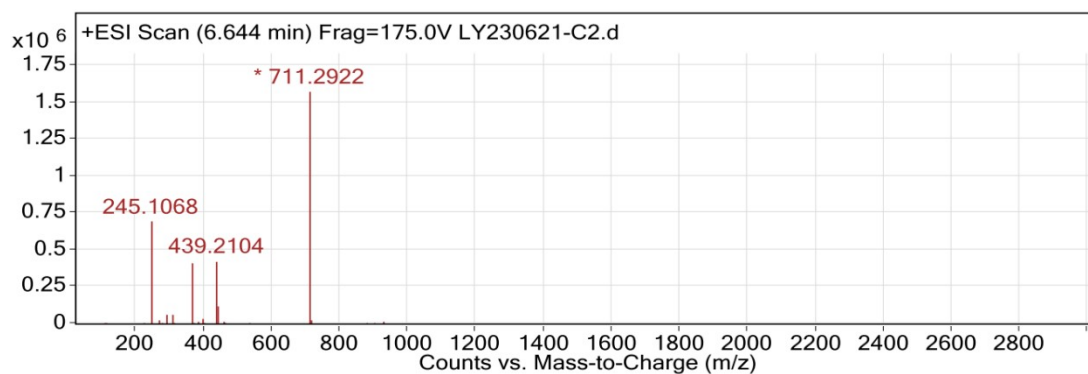
HRMS spectra of **SiR-N8C**



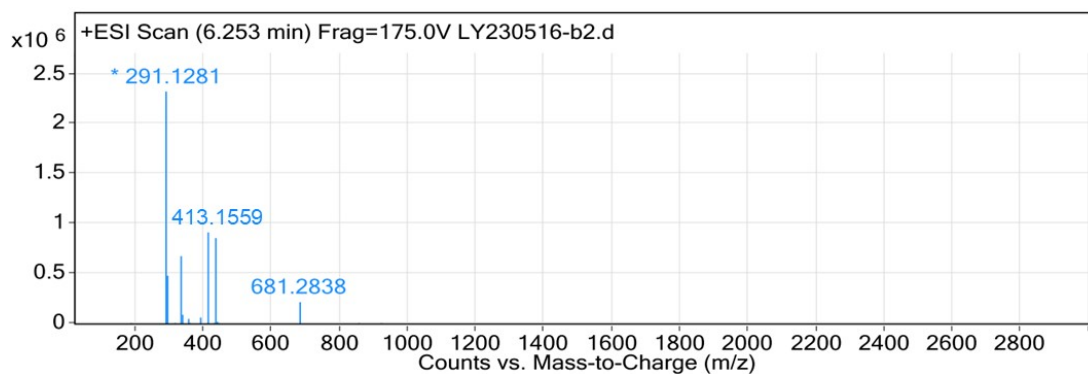
HRMS spectra of **SiR-N12C**



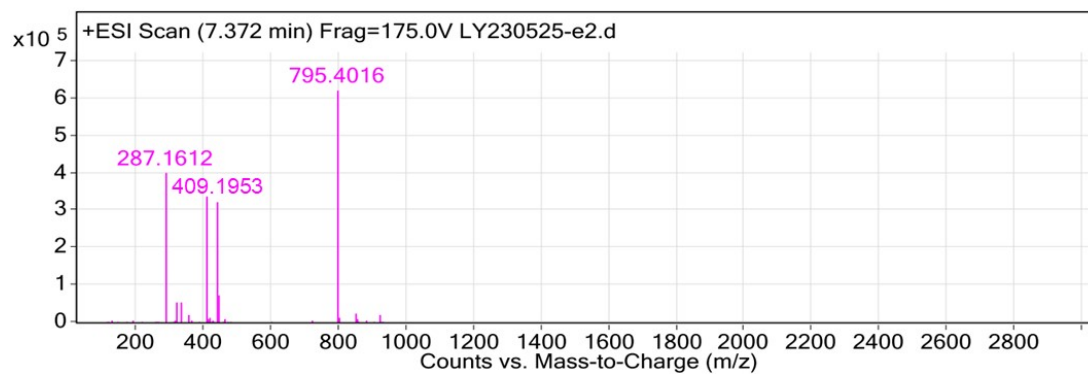
HRMS spectra of **6**



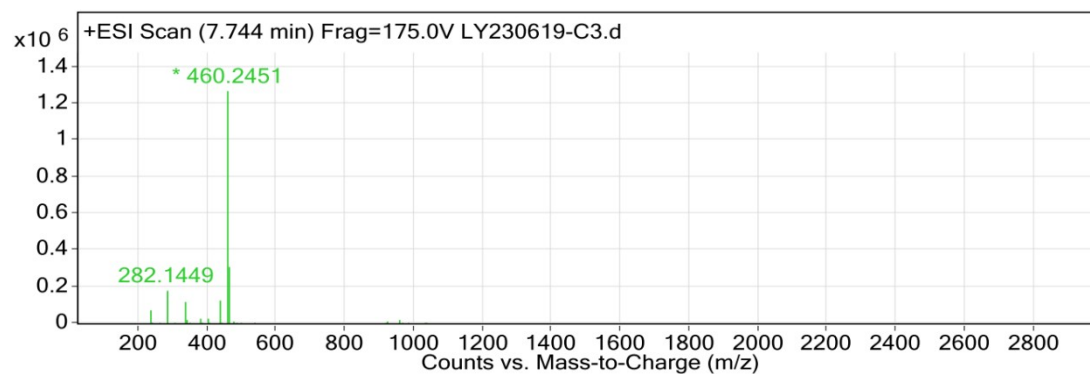
HRMS spectra of **7**



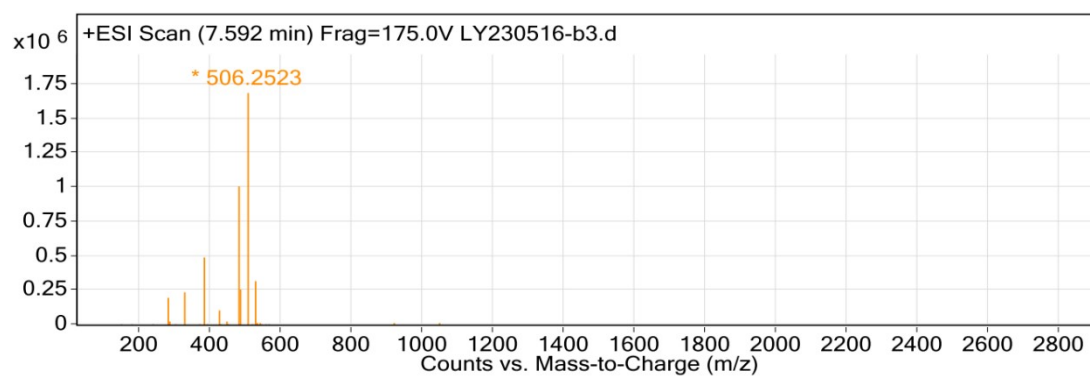
HRMS spectra of **8**



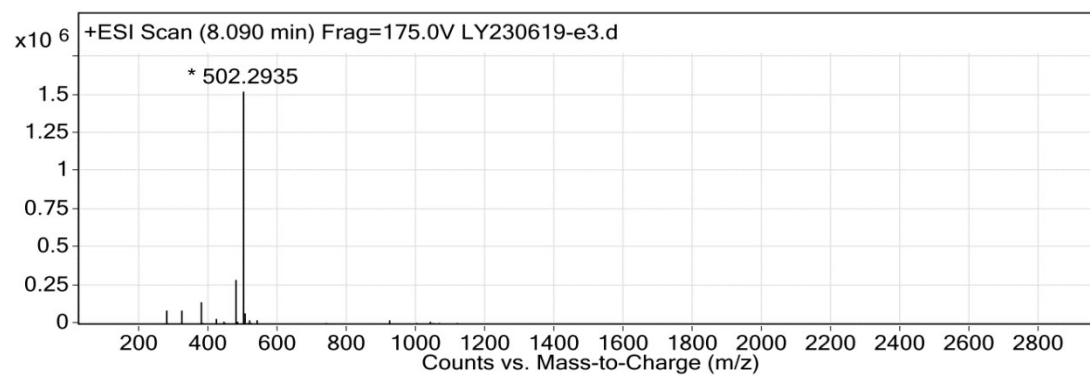
HRMS spectra of **10**



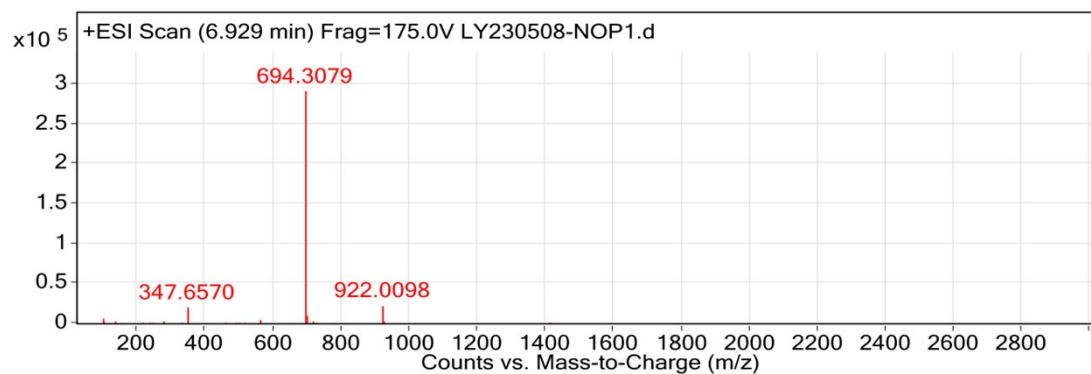
HRMS spectra of **11**



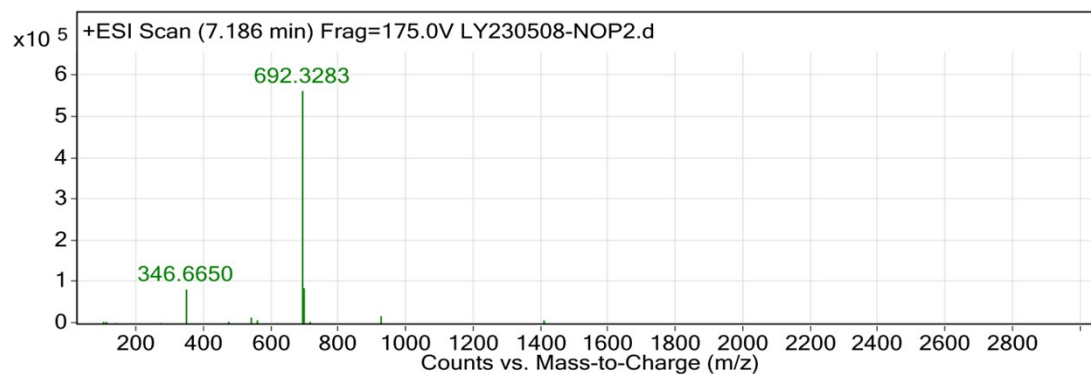
HRMS spectra of **12**



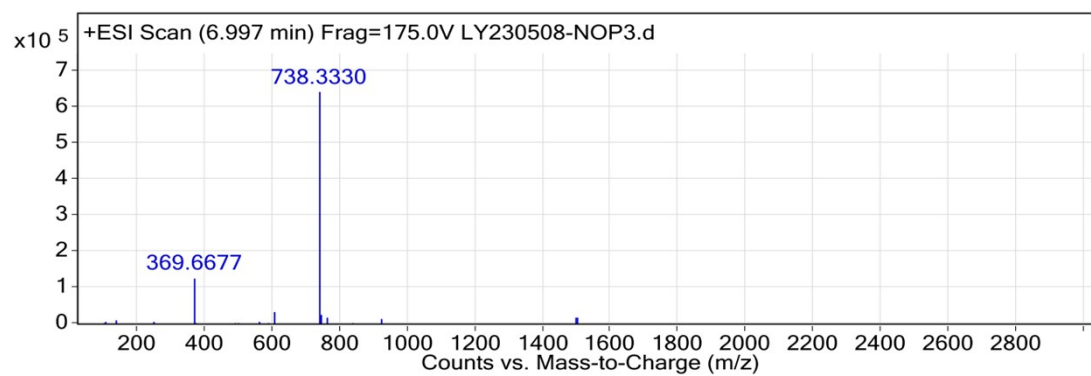
HRMS spectra of **NOP-1**



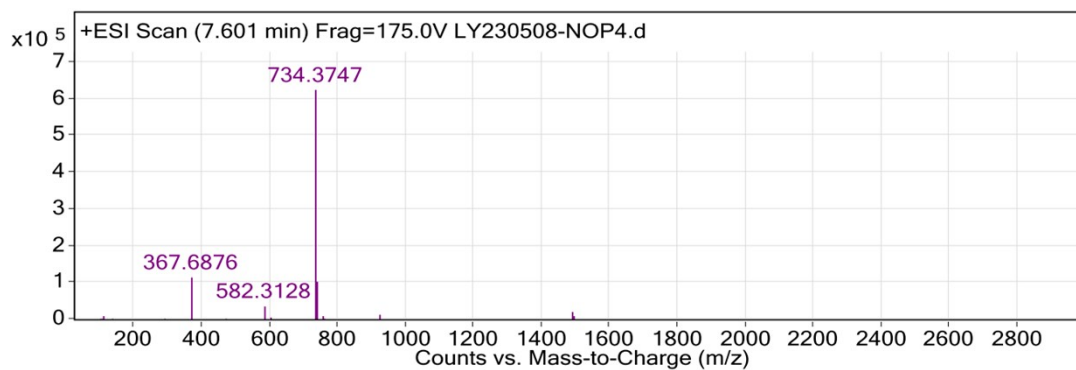
HRMS spectra of **NOP-2**



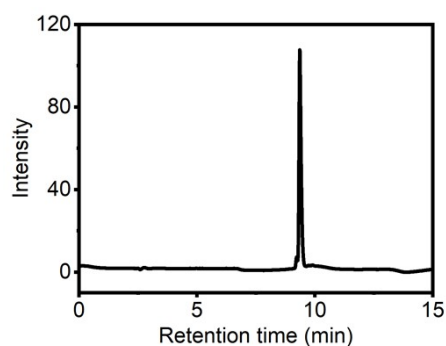
HRMS spectra of **NOP-3**



HRMS spectra of **NOP-4**

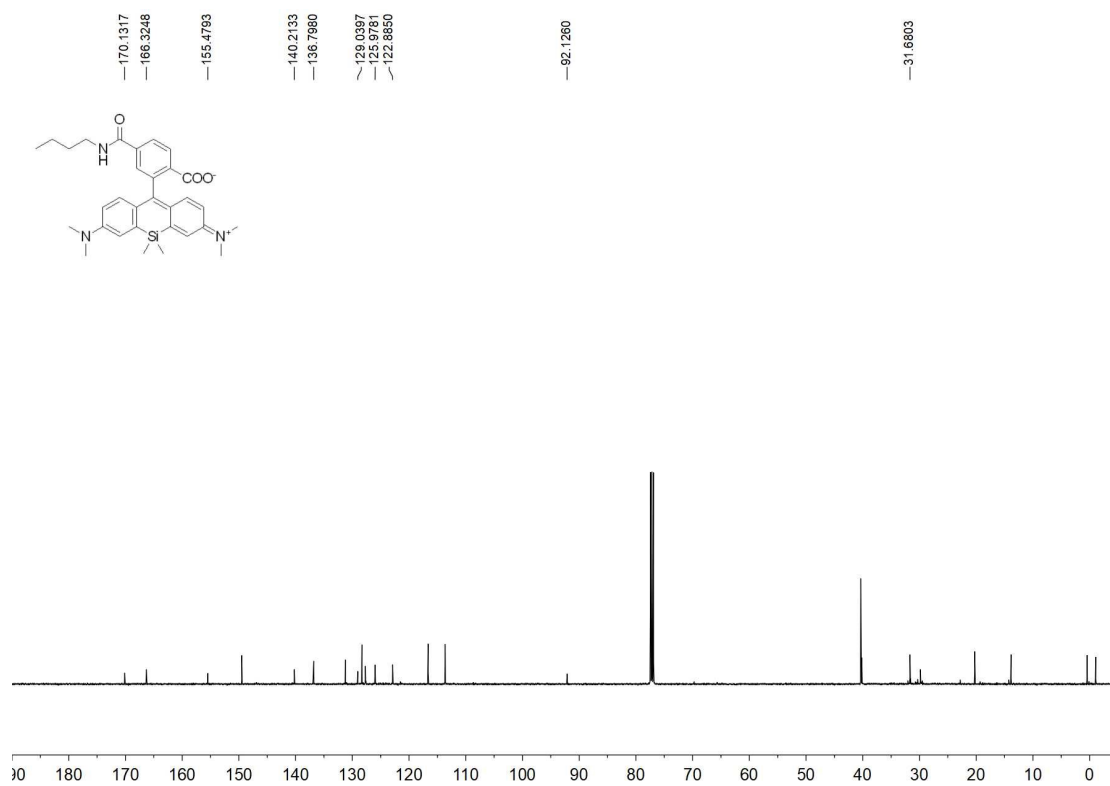
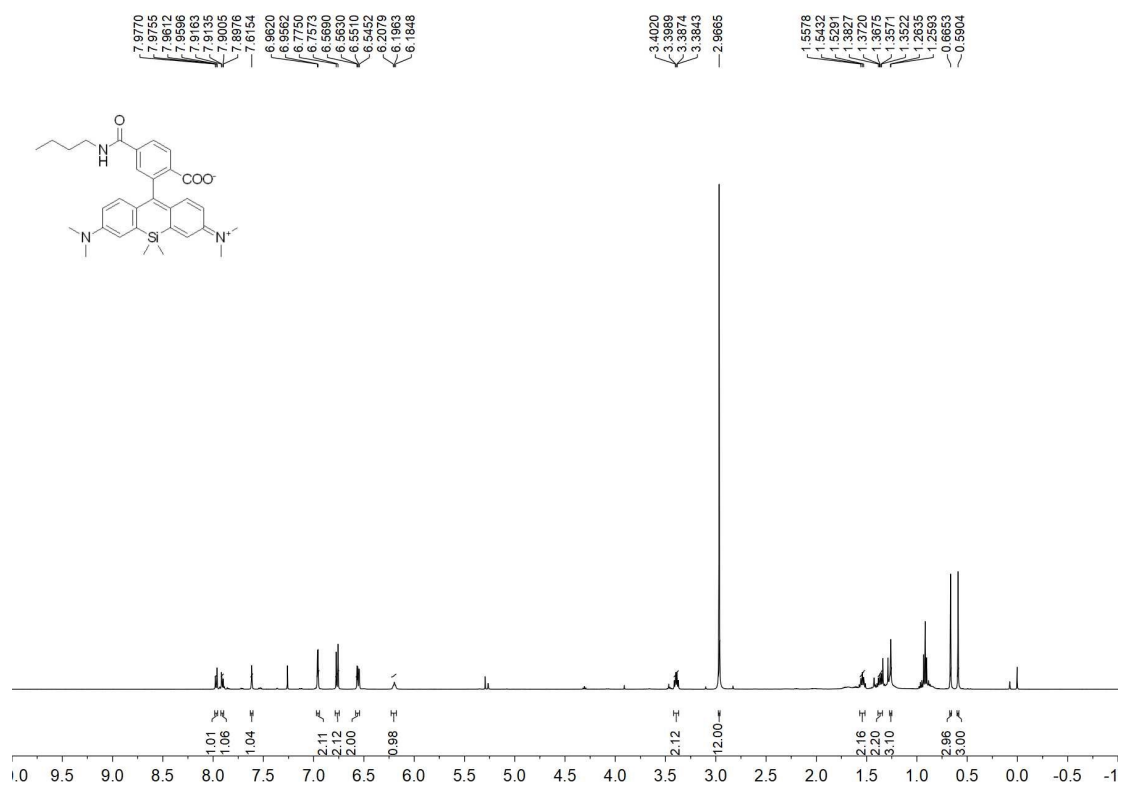


HPLC trace of **NOP-1**

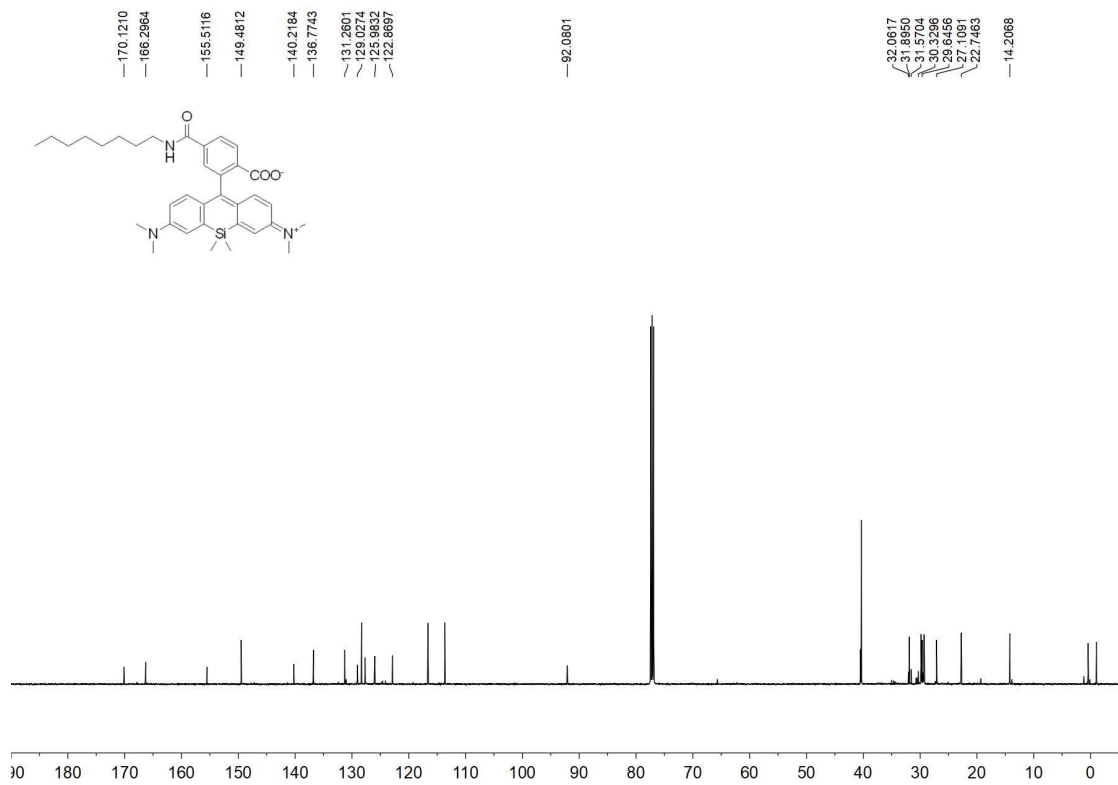
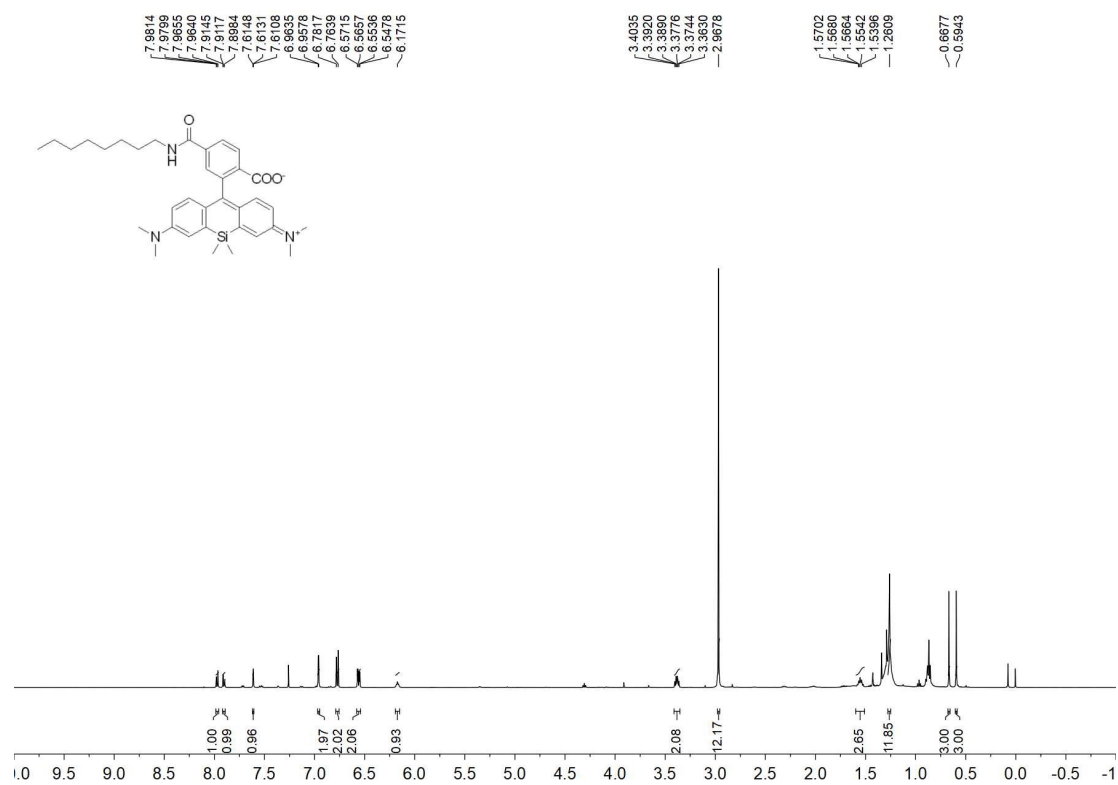


The purity of **NOP-1** was verified by High Performance Liquid Chromatography (HPLC). **NOP-1** (100 μ M) dissolved in methanol was analyzed by HPLC on an Agilent Technologies 1260 Infinity system. The mobile phase A: 1% CF_3COOH in distilled water. The mobile phase B: MeOH. Running time: 0-3 min, 95% phase A + 5% phase B; 3-7 min, 95% phase A + 5% phase B \rightarrow 5% phase A + 95% phase B; 7-10 min, 5% phase A + 95% phase B; 10-13 min, 5% phase A + 95% phase B \rightarrow 5% phase A + 95% phase B; 13-15 min, 5% phase A + 95% phase B. Flow rate: 1 mL/min. Detection wavelength: 256 nm. Column: Ultimate[®]XB-C18, 5 μ m, 4.6 \times 250 mm.

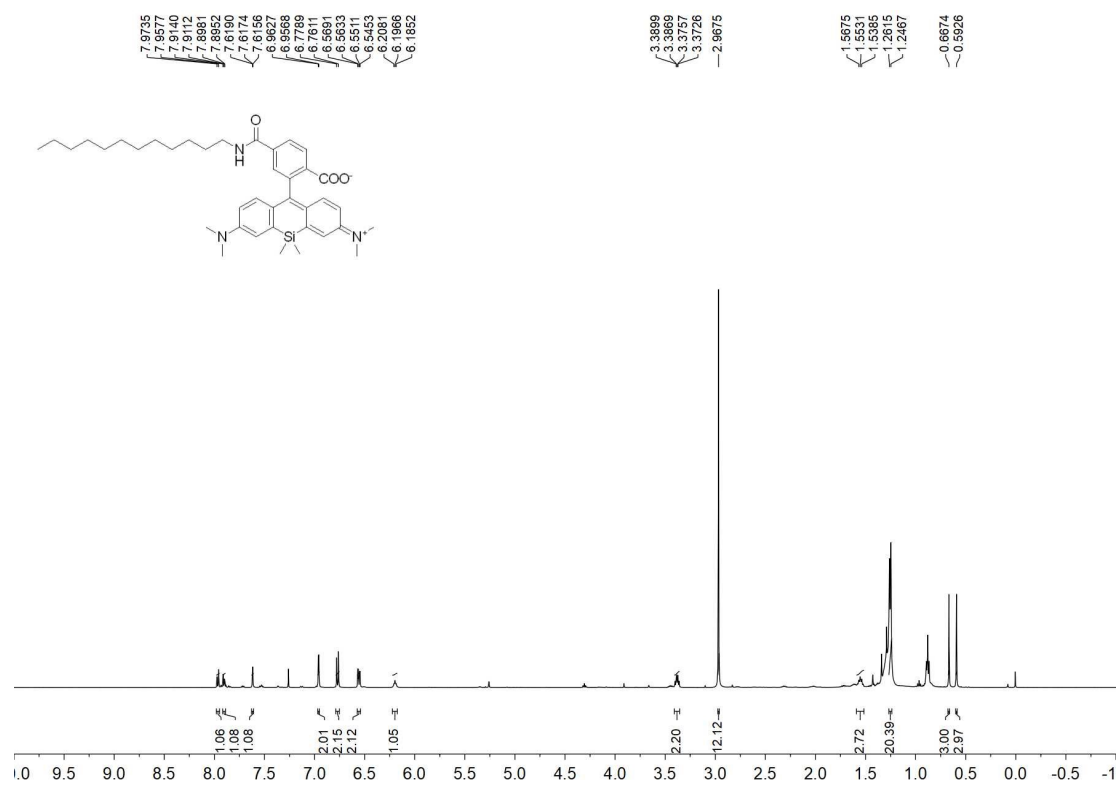
¹H NMR and ¹³C NMR of SiR-N4C



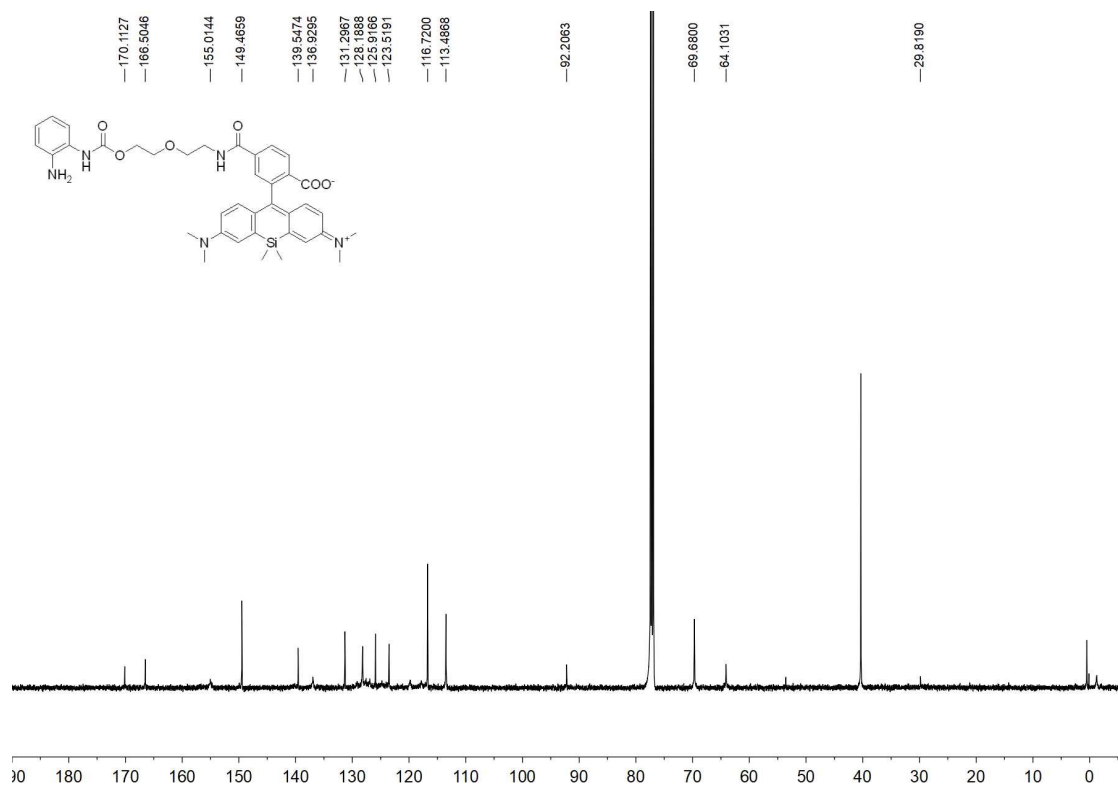
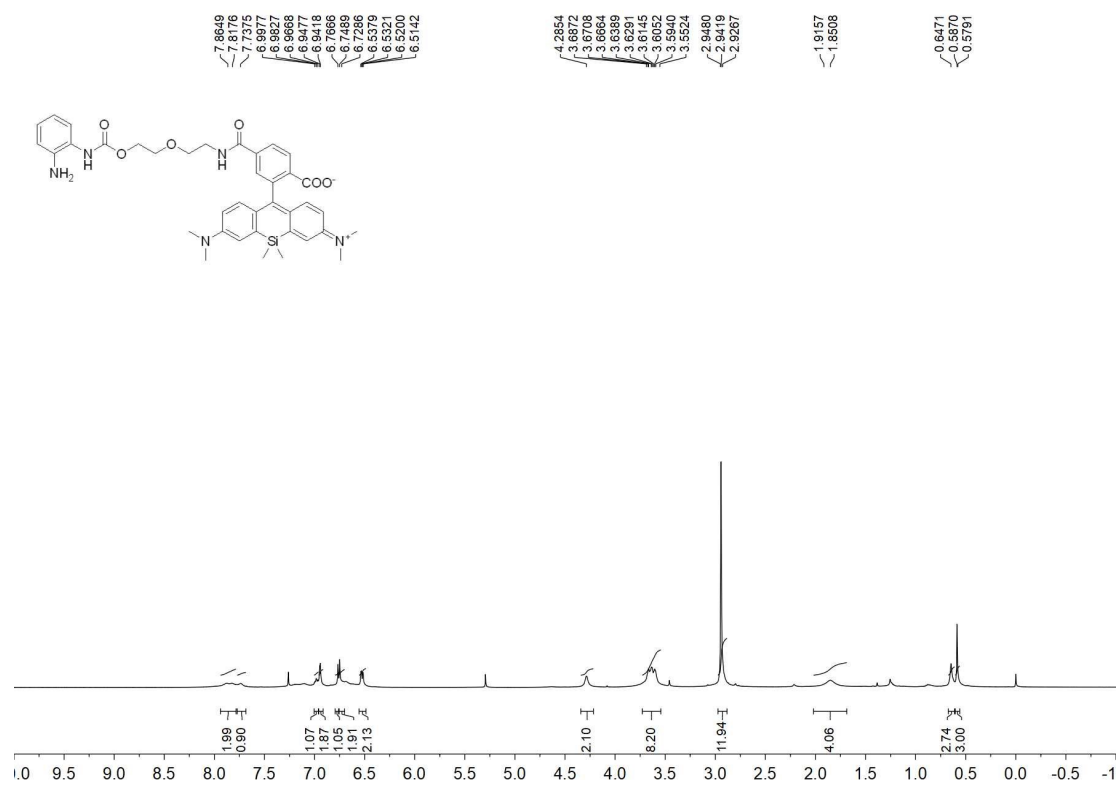
¹H NMR and ¹³C NMR of SiR-N8C



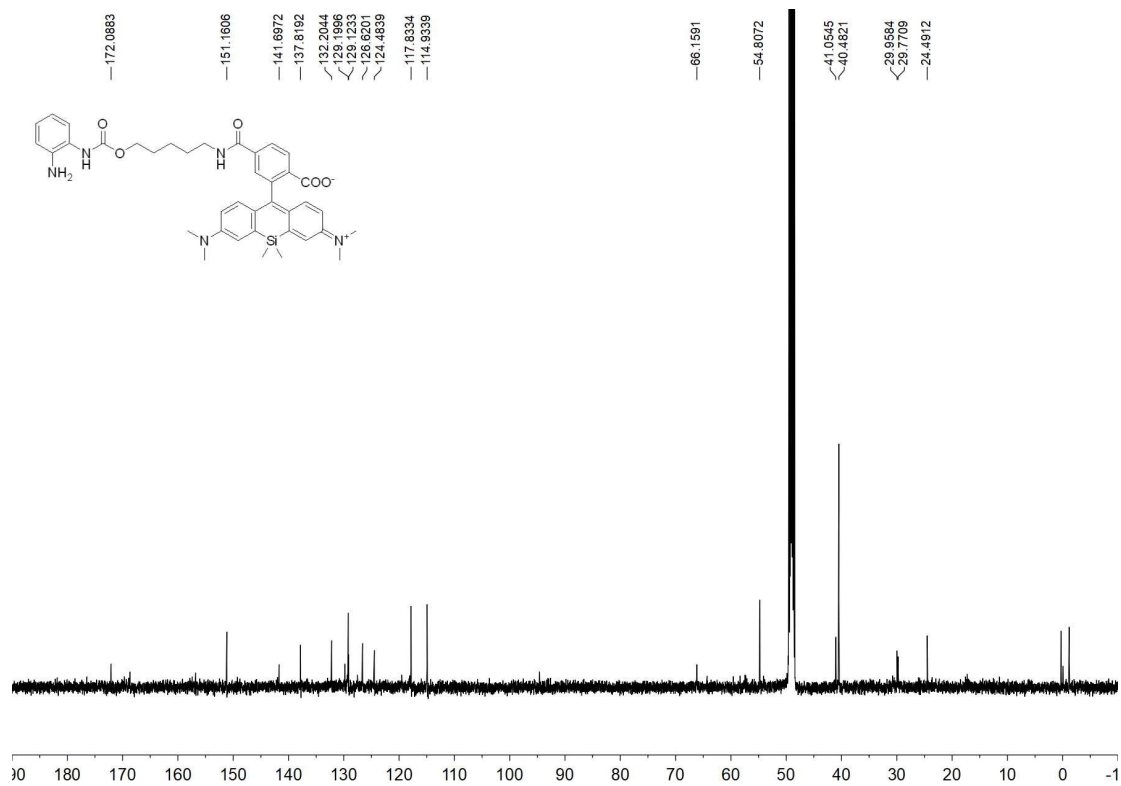
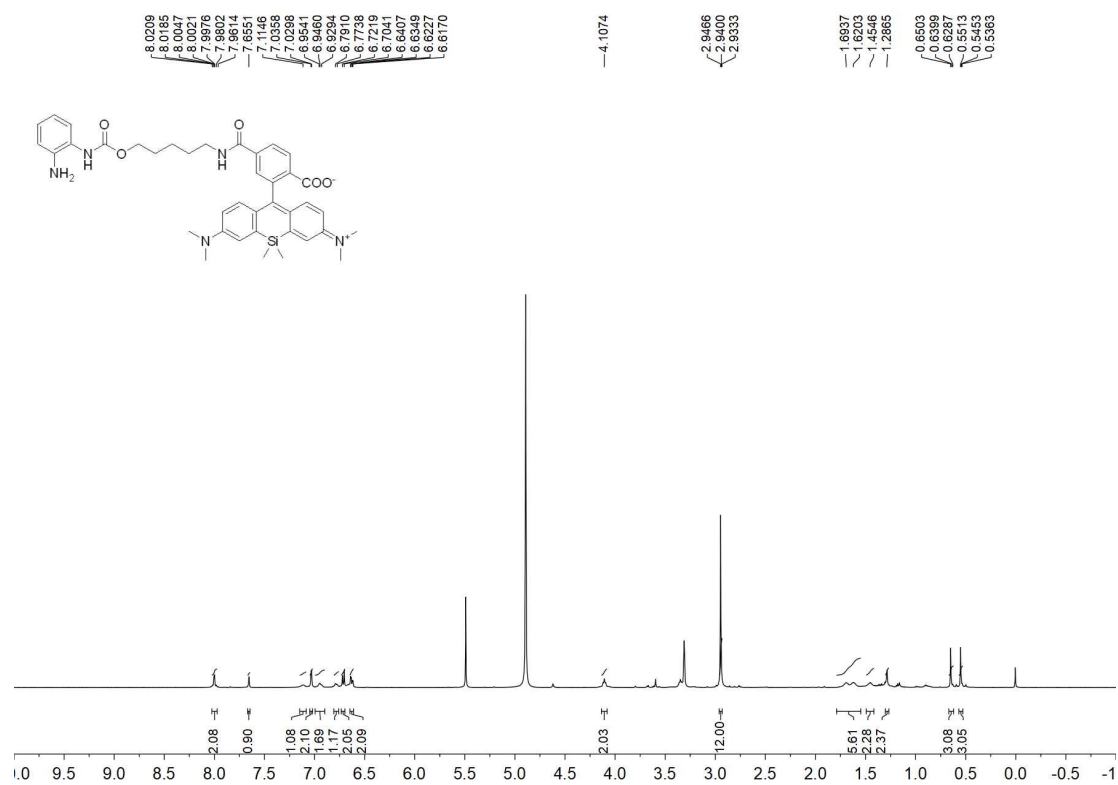
¹H NMR and ¹³C NMR of SiR-N12C



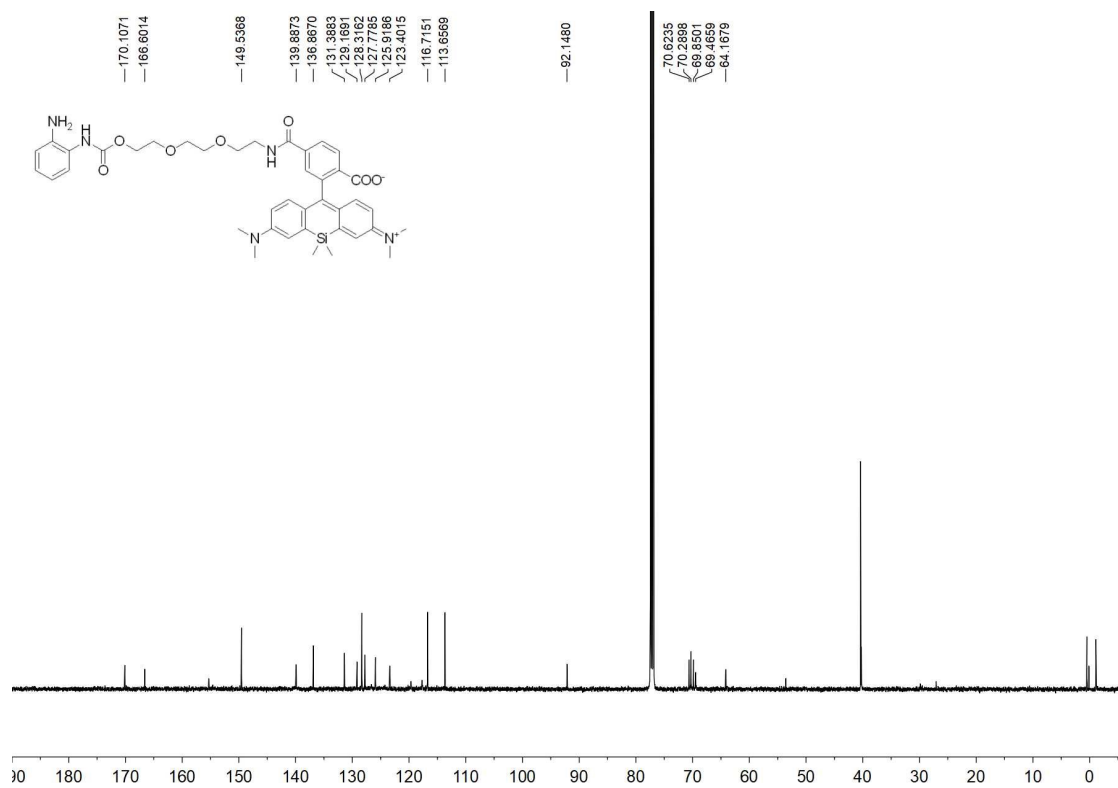
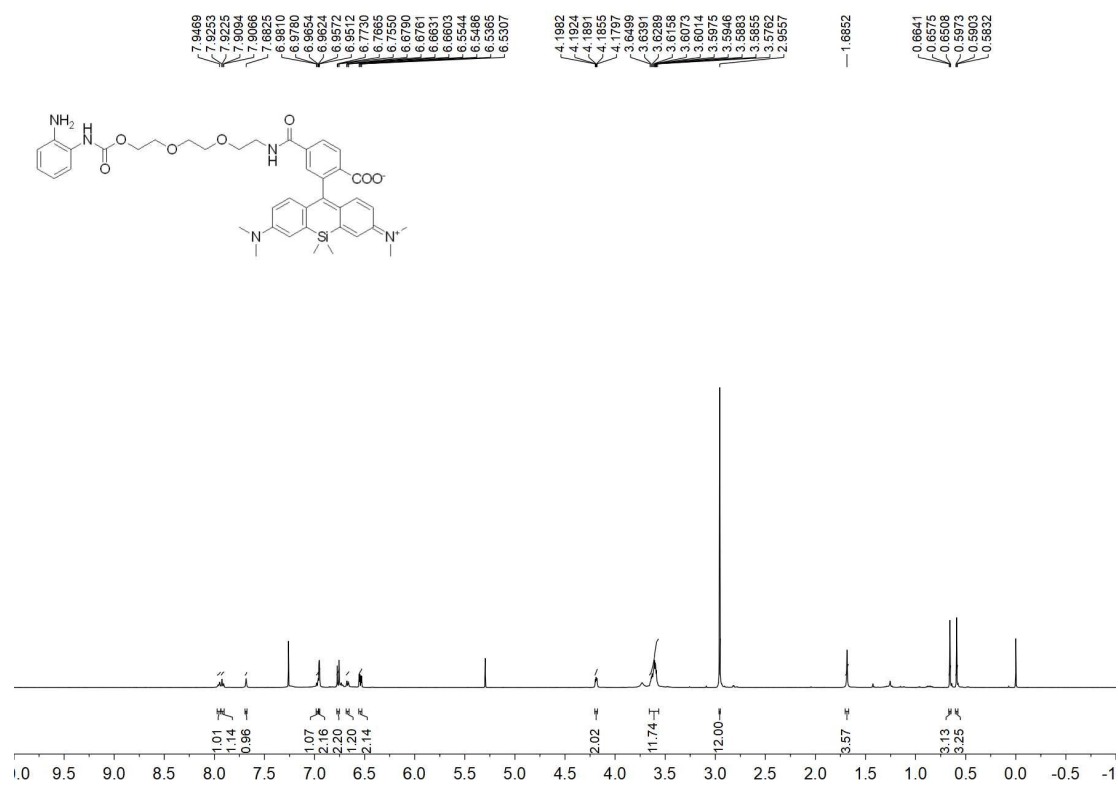
¹H NMR and ¹³C NMR of NOP-1



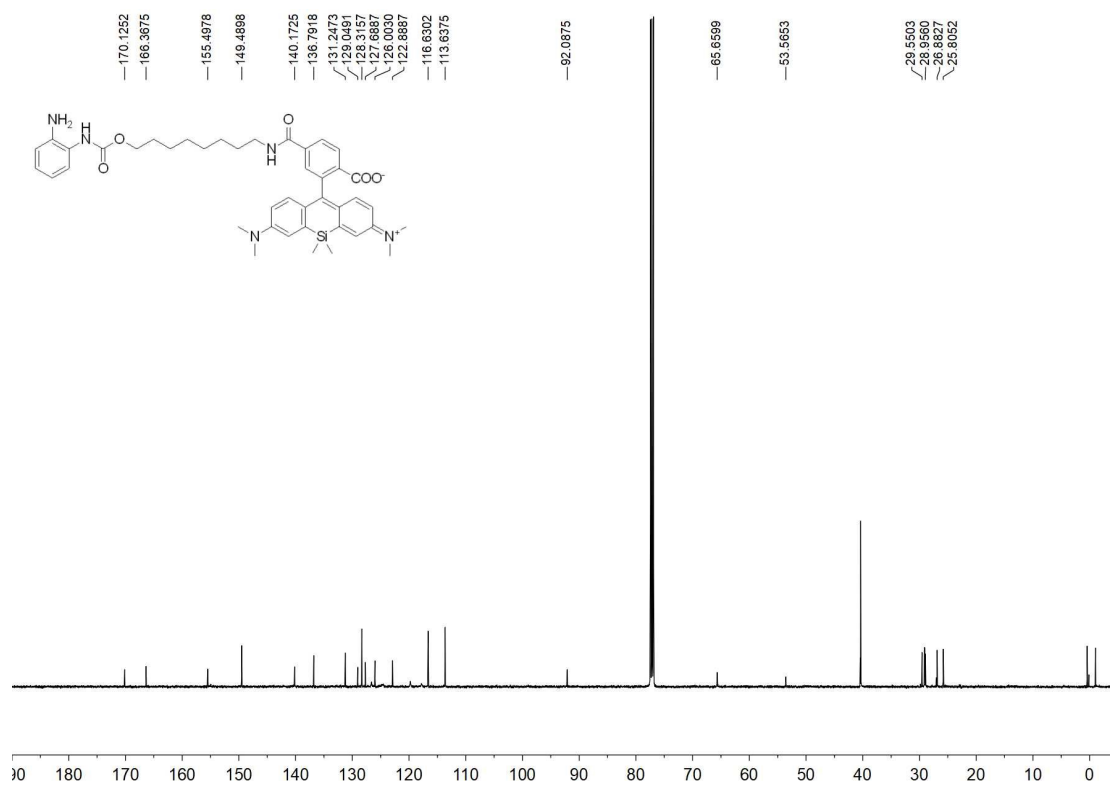
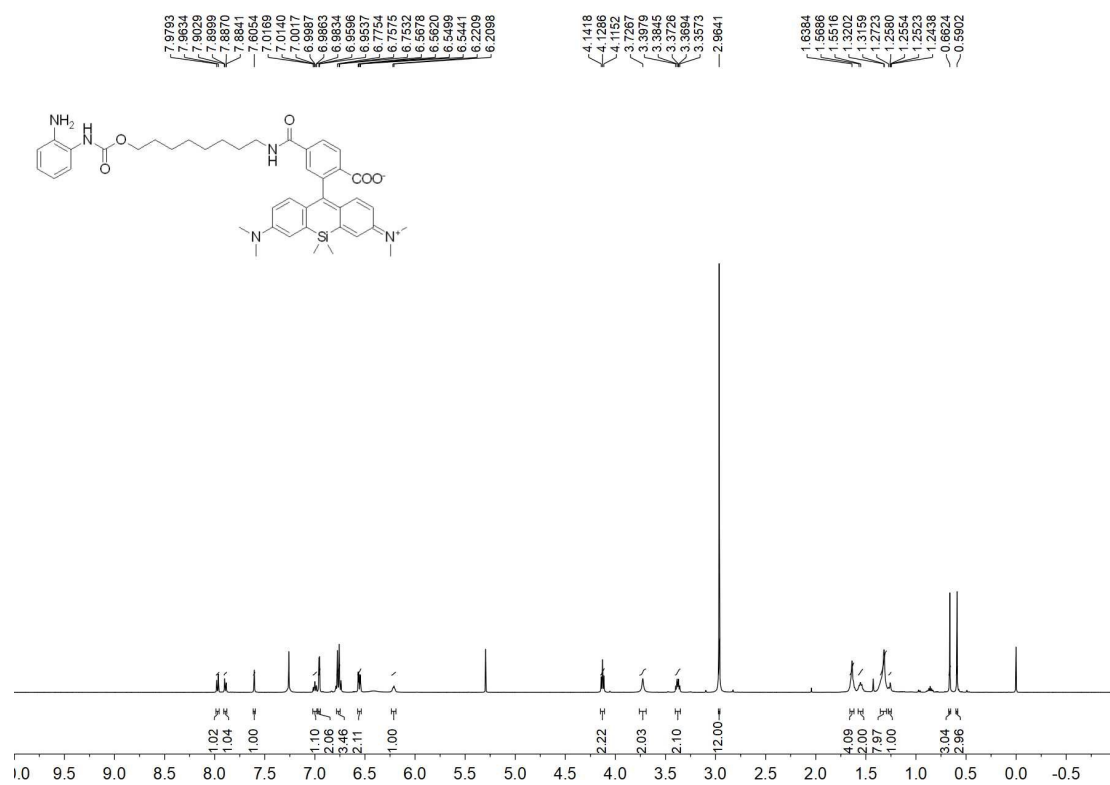
¹H NMR and ¹³C NMR of NOP-2



¹H NMR and ¹³C NMR of NOP-3



¹H NMR and ¹³C NMR of NOP-4



References

1. K. Kyrylkova, S. Kyryachenko, M. Leid and C. Kioussi, *Methods Mol Biol*, 2012, **887**, 41-47.
2. G. Lukinavičius, K. Umezawa, N. Olivier, A. Honigmann, G. Yang, T. Plass, V. Mueller, L. Reymond, I. R. Corrêa, Jr., Z. G. Luo, C. Schultz, E. A. Lemke, P. Heppenstall, C. Eggeling, S. Manley and K. Johnsson, *Nat Chem*, 2013, **5**, 132-139.